

RESEARCH ARTICLE

New roles of NO TRANSMITTING TRACT and SEEDSTICK during medial domain development in *Arabidopsis* fruits

Humberto Herrera-Ubaldo¹, Paulina Lozano-Sotomayor^{1,*}, Ignacio Ezquer², Maurizio Di Marzo², Ricardo Aarón Chávez Montes¹, Andrea Gómez-Felipe¹, Jeanneth Pablo-Villa¹, David Diaz-Ramirez³, Patricia Ballester⁴, Cristina Ferrándiz⁴, Martin Sagasser⁵, Lucia Colombo², Nayelli Marsch-Martínez³ and Stefan de Folter^{1,‡}

ABSTRACT

The gynoecium, the female reproductive part of the flower, is key for plant sexual reproduction. During its development, inner tissues such as the septum and the transmitting tract tissue, important for pollen germination and guidance, are formed. In *Arabidopsis*, several transcription factors are known to be involved in the development of these tissues. One of them is NO TRANSMITTING TRACT (NTT), essential for transmitting tract formation. We found that the NTT protein can interact with several gynoecium-related transcription factors, including several MADS-box proteins, such as SEEDSTICK (STK), known to specify ovule identity. Evidence suggests that NTT and STK control enzyme and transporter-encoding genes involved in cell wall polysaccharide and lipid distribution in gynoecial medial domain cells. The results indicate that the simultaneous loss of NTT and STK activity affects polysaccharide and lipid deposition and septum fusion, and delays entry of septum cells to their normal degradation program. Furthermore, we identified *KAWAK*, a direct target of NTT and STK, which is required for the correct formation of fruits in *Arabidopsis*. These findings position NTT and STK as important factors in determining reproductive competence.

KEY WORDS: NO TRANSMITTING TRACT, SEEDSTICK, Fruit, Gynoecium, Medial domain, Septum, Cell wall, Lipids, Polysaccharide, *KAWAK*

INTRODUCTION

A large part of our food comes from floral parts, fruits and seeds. Therefore, a deep understanding of the regulatory networks guiding the developmental processes of these structures and tissues is important. Flowering species mostly give rise to the pistil, or so-called gynoecium, in the center of the flower. The gynoecium, from a biological point of view, is essential for plant

reproduction. In general, at the apical end it has a stigma to facilitate pollen capture and germination, and the stigma is connected via the style to the ovary where the ovules will be formed. The transmitting tract facilitates pollen tube growth through the style and the ovary, and, upon fertilization inside each ovule, seed development starts. The gynoecium is now called a fruit, which increases rapidly in size owing to hormones produced by the seeds (Roeder and Yanofsky, 2006; Alvarez-Buylla et al., 2010; Ferrándiz et al., 2010; Sotelo-Silveira et al., 2013; Marsch-Martínez and de Folter, 2016).

In *Arabidopsis*, the correct formation of the medial domain in the gynoecium is a key process for female reproductive competence and seed formation. This domain includes placental tissues and ovules, and the structures that capture the pollen grains and guide pollen tubes to reach the ovules and, therefore, facilitate fertilization. These structures and tissues, including stigma, style, septum and transmitting tract, are also known as the marginal tissues (Fig. 1A). These tissues arise from the carpel margin meristem (CMM) (Bowman et al., 1999; Alvarez and Smyth, 2002; Nole-Wilson et al., 2010; Wynn et al., 2011; Reyes-Olalde et al., 2013), a meristematic tissue that emerges as two internal ridges (termed medial ridges) in the young gynoecium (Fig. 1A), which fuse together when they reach each other in the middle of the gynoecium, thereby forming the septum. This postgenital fusion occurs at stage 9 of gynoecium development (Bowman et al., 1999; Roeder and Yanofsky, 2006). Ovule primordia can be seen at stage 9 (Bowman et al., 1999; Roeder and Yanofsky, 2006; Reyes-Olalde et al., 2013). At stage 11, the gynoecium fully closes and the stigma is then fully developed. During stage 12, the style and the transmitting tract differentiate, and at stage 13 the gynoecium is fully mature (Smyth et al., 1990; Bowman et al., 1999; Roeder and Yanofsky, 2006; Reyes-Olalde et al., 2013).

Over 80 genes have been identified as regulators of medial domain development, mainly participating at stages 9 to 11 (Reyes-Olalde et al., 2013). For instance, in the case of the postgenital fusion of the medial ridges, the basic helix-loop-helix (bHLH) gene *SPATULA* (*SPT*) has been found to be an important player (Alvarez and Smyth, 1999, 2002; Heisler et al., 2001; Reyes-Olalde et al., 2017). The formation of the stigma and style is controlled by *NGATHA* (*NGA*), *STYLISH* (*STY*) and *HECATE* (*HEC*) genes (Gremski et al., 2007; Alvarez et al., 2009; Trigueros et al., 2009). *SEEDSTICK* (*STK*) directs ovule specification, funiculus development, and seed abscission (Favaro et al., 2003; Pinyopich et al., 2003; Balanzà et al., 2016). Fertilization is a key process for sexual reproduction, and an important point in this process is that the pollen tubes can reach the ovules. The synergid cells, in the embryo sac inside the ovule, produce signals to attract the pollen tube (Mizuta and Higashiyama, 2018). For pollen tubes

¹Unidad de Genómica Avanzada (LANGEBIO), Centro de Investigación y de Estudios Avanzados del Instituto Politécnico Nacional (CINVESTAV-IPN), Irapuato 36824, Guanajuato, México. ²Dipartimento di Bioscienze, Università degli Studi di Milano, Milan 20133, Italy. ³Departamento de Biotecnología y Bioquímica, Unidad Irapuato, CINVESTAV-IPN, Irapuato 36824, Guanajuato, México. ⁴Instituto de Biología Molecular y Celular de Plantas, CSIC-UPV Universidad Politécnica de Valencia, 46022, Spain. ⁵Bielefeld University, Faculty of Biology, Chair of Genetics and Genomics of Plants, Bielefeld 33615, Germany.

*Present address: Departamento de Química, División de Ciencias Naturales y Exactas, Universidad de Guanajuato, Guanajuato, México.

‡Author for correspondence (stefan.defolter@cinvestav.mx)

© H.H., 0000-0002-5408-4022; P.L., 0000-0002-3933-0002; I.E., 0000-0003-1886-0095; M.D., 0000-0001-9045-8370; J.P., 0000-0003-3134-5901; N.M., 0000-0001-9522-0062; S.d.F., 0000-0003-4363-7274

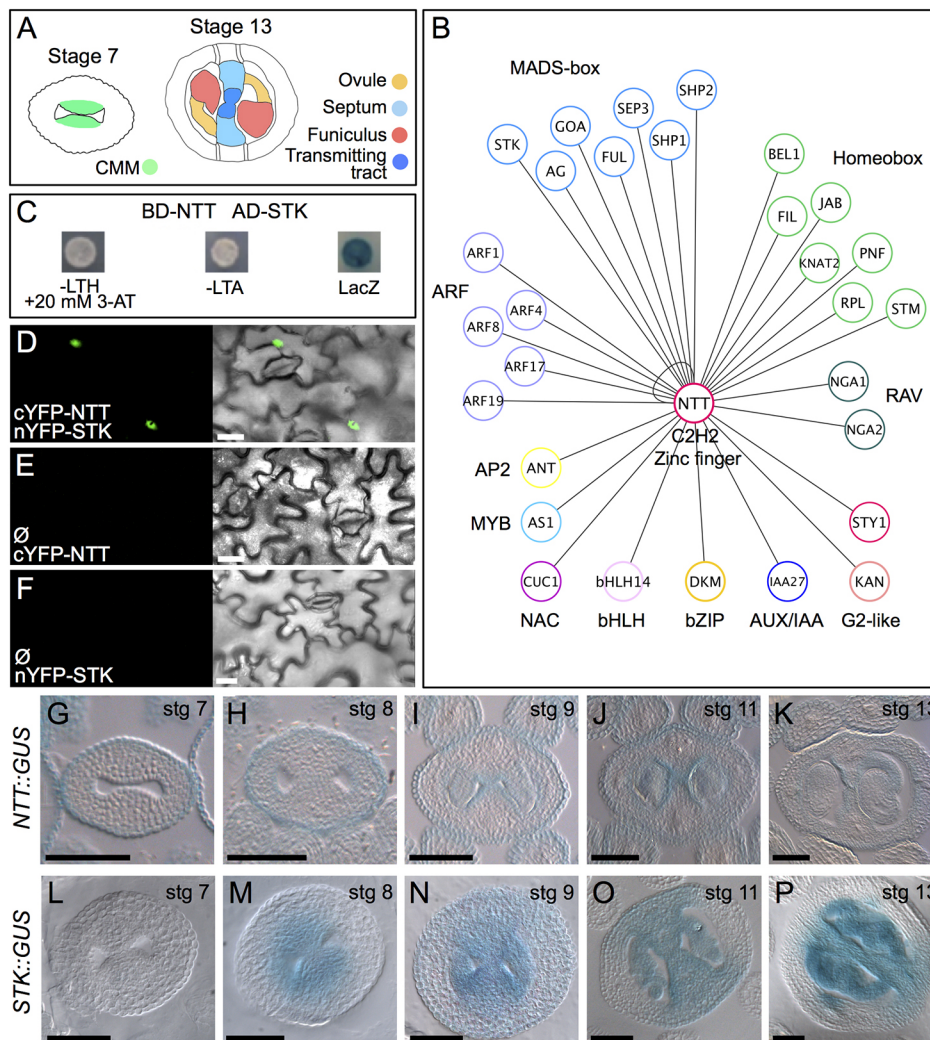


Fig. 1. NTT and STK physically interact and are co-expressed in the gynoecium medial domain. (A) Schematic of the medial domain in stage 7 and 13 gynoecium; the CMM gives rise to all medial tissues present at stage 13: septum, transmitting tract, funiculus and ovules. (B) NTT protein interactions (lines represent interactions) based on a Y2H assay. (C) Y2H assay of the NTT-STK combination for the three reporter genes, showing positive results. (D-F) BiFC assay in tobacco leaves for *STK-NTT* (D) and negative controls with empty vectors (E,F). (G-P) *NTT::GUS* (G-K) and *STK::GUS* (L-P) in transverse gynoecia sections at different stages. Scale bars: 20 μ m in D-F; 50 μ m in G-P.

to reach the ovules, cell wall modifications have to take place (Crawford and Yanofsky, 2008; Dresselhaus and Franklin-Tong, 2013). On the female side, these modifications take place when the transmitting tract forms. Cells in this tissue produce an extracellular matrix (ECM) containing glycoproteins, glycolipids and polysaccharides that facilitates pollen tube growth (Lennon et al., 1998; Crawford and Yanofsky, 2008). A genetic pathway controlling transmitting tract formation includes the three redundant bHLH *HEC* transcription factors (Gremski et al., 2007), the *HALF FILLED (HAF)* gene (also known as *CESTA, CES*), which acts redundantly with the closely related *BRASSINOSTEROID ENHANCED EXPRESSION 1 (BEE1)* and *BEE3* genes (Crawford and Yanofsky, 2011), and the zinc-finger transcription factor *NO TRANSMITTING TRACT (NTT)*, which controls this process in the ovary but not in the style (Crawford and Yanofsky, 2011). All these genes contribute to ECM production and programmed cell death (Crawford et al., 2007; Crawford and Yanofsky, 2011). Furthermore, other genes expressed in the style and transmitting tract encode enzymes that modify cell walls (Dresselhaus and Franklin-Tong, 2013), e.g. beta-1,3-glucanases (Delp and Palva, 1999). On the male side, growing pollen tubes secrete cell wall-degrading enzymes that help pollen tubes on their way through the pistil (Mollet et al., 2013; Hepler et al., 2013), e.g. the pectin methylesterase *VANGUARD1 (VGD1)* (Jiang et al., 2005).

The NTT transcription factor, besides its role in transmitting tract formation, is also important for root meristem development (Crawford et al., 2015), and during fruit development NTT is involved in valve margin formation (Chung et al., 2013) and replum development (Marsch-Martínez et al., 2014). In the latter report, we detected protein-protein interactions between NTT and other fruit-related transcription factors, including some MADS-box proteins such as SHATTERPROOF1 (SHP1) and SHP2.

The MADS-box transcription factor STK has been well-characterized in ovule and funiculus development, and is involved in ovule identity determination together with SHP1 and SHP2 (Colombo et al., 1995; Favaro et al., 2003; Pinyopich et al., 2003). Furthermore, it has been shown that STK participates in seed development by controlling secondary metabolism (Mizzotti et al., 2012, 2014), cell wall properties (Ezquer et al., 2016) and seed abscission (Balanzà et al., 2016). Here, we report NTT protein interaction with STK and describe novel roles for NTT and STK during medial domain development, further demonstrating that they are important for the reproductive competence of *Arabidopsis* plants. Our results indicate that NTT and STK are involved in the control of early events of gynoecium development, such as septum fusion, septum cell integrity, impact fertilization efficiency and seed-set, and affect senescence after fertilization. They control genes involved in carbohydrate metabolism and lipid distribution in septum cell walls.

RESULTS

The NTT and STK proteins interact

We recently reported that the transcription factor NO TRANSMITTING TRACT (NTT) promotes replum development, and that it interacts in the yeast two-hybrid (Y2H) system with proteins related to fruit development such as FRUITFULL (FUL), REPLUMLESS (RPL), SHP1, SHP2 and SHOOT MERISTEMLESS (STM) (Marsch-Martínez et al., 2014). We expanded this interaction survey with a uni-directional Y2H screen (see Materials and Methods) and found that NTT was able to interact with an additional 24 transcription factors (Fig. 1B; Table S1), suggesting that NTT fulfils various roles by forming part of different protein complexes. Of particular interest is the fact that NTT interacted with all MADS-box proteins tested.

In this work, we focused on the interaction of NTT with the MADS-box protein SEEDSTICK (STK), which is known to provide the D-function for ovule identity (Favaro et al., 2003; Pinyopich et al., 2003). In the Y2H assay, the combination NTT-STK activated all three reporter genes (*HIS3*, *ADE* and *lacZ*), indicating that these proteins are able to interact (Fig. 1C).

To confirm this Y2H result, a bimolecular fluorescence complementation assay (BiFC; Fig. 1D-F) was performed. For this, NTT was fused to the cYFP and STK fused to nYFP region, and fluorescence from the reconstituted YFP was detected in leaf cells (Fig. 1D), indicating that the two proteins interact *in planta*, confirming the Y2H result. Fluorescence was observed in the nucleus, in agreement with the expected localization of transcription factors.

NTT and STK are co-expressed during gynoecium development

The Y2H and BiFC assays suggested that NTT and STK could be interacting during gynoecia development in *Arabidopsis*, as both participate in this process. In order to visualize those regions where these proteins could be acting together, we analyzed transverse thin sections of stage 7 to stage 13 gynoecia of the reporter lines *NTT::GUS* and *STK::GUS* (Kooiker et al., 2005).

Activity of the *NTT* promoter was detected from stage 9 to 13 gynoecia in the medial domain (Fig. 1I-K), as reported before (Crawford et al., 2007; Chung et al., 2013; Marsch-Martínez et al., 2014). The activity of the *STK* promoter was visible in the medial domain from stage 8 till stage 13 gynoecia (Fig. 1M-P). Blue staining was observed in the medial domain in ovule primordia and later in ovules and the septum (Fig. 1N-P), in agreement with previous reports (Kooiker et al., 2005; Losa et al., 2010). In summary, based on the two promoter activity analyses, *NTT* and *STK* are co-expressed during gynoecium development, specifically in medial domain tissues. These results support the possibility of the formation of a dimer or higher-order complex containing NTT and STK in these tissues.

Constitutive expression of NTT together with STK affects flower development

We showed that NTT can physically interact with STK, and that the genes are co-expressed in the medial domain of the gynoecium. Subsequently, we wanted to explore the biological relevance of this putative NTT-STK protein dimer or complex during *Arabidopsis* flower development. The first approach we took was to generate double constitutive expression plants, assuming that this would increase the accumulation of the NTT-STK protein complex in the plant. For this, we crossed a *35S::NTT* line (Marsch-Martínez et al., 2014) with a *35S::STK* line (Favaro et al., 2003) and we analyzed

the F1 generation. Fertility is affected in the single *35S::NTT* line, although this line is still able to produce some seeds (Marsch-Martínez et al., 2014). The *35S::STK* line flowers early with respect to wild type and develops small flowers with reduced fertility (Favaro et al., 2003). Interestingly, in double constitutive *35S::NTT 35S::STK* plants, reproductive development was severely affected (Fig. S1), and the phenotypic alterations were stronger with respect to those observed in the single constitutive expression lines. In general, plants were very small, and when the first flowers reached around floral stage 10, an arrest of floral development was observed and flowers began to senesce. The formed flowers were male and female sterile and, as a consequence, we never observed fruit development, in contrast to the two single constitutive expression lines (Fig. S1). These results show that increased levels of the possible NTT-STK complex can severely affect flower development, suggesting that they may work together in the plant.

The *ntt stk* double mutant is affected in gynoecium medial domain development

To understand better the biological role of the NTT-STK interaction, and to unravel new putative roles for these transcription factors, we generated an *ntt stk* double mutant. Fruits of the double mutant presented some phenotypes that were a combination of those observed in the single mutants, such as smaller fruits, fewer seeds, no transmitting tract, larger funiculi, irregular seed spacing, lack of seed abscission and reduced seed size (Fig. 2A-D; Fig. 3A,B,G,H) (Pinyopich et al., 2003; Crawford et al., 2007). Interestingly, new phenotypes were observed in the *ntt stk* double mutant, all related to septum development. First, septum fusion defects were observed in 16% of the fruits ($n=360$), a phenotype never observed in either single mutant (*ntt* $n=106$, *stk* $n=121$), nor in wild-type fruits ($n=49$) (Fig. 2A-E). These septum fusion defects were observed as holes (up to three holes) in the septum of a fruit. In the most severe cases, the septum fusion defects could be seen along 60% of the length of the fruit (Fig. 2E). Furthermore, alteration in septum fusion was also observed at stage 14 as a longitudinal division line (furrow) in the middle of the septum, which corresponds to the place where the two septum primordia meet and normally fuse during wild-type gynoecium development (Fig. 2F,G). This latter phenotype was observed in most of the *ntt stk* fruits.

A second phenotype observed was related to the aspect of septum cells. When the septum of stage 14 fruits was inspected using scanning electron microscopy (SEM), septum cell integrity in *ntt stk* fruits appeared to be preserved (Fig. 2G,I). In contrast, septum cells in wild-type fruits at the same stage presented signs of degeneration and collapse (Fig. 2F,H).

As septum development continues, at stage 15, generalized degradation and holes can be observed in the medial domain of wild-type, *ntt* and *stk* single mutant fruits (Fig. 2J-L). Strikingly, in the *ntt stk* double mutant no cell degradation in this region was observed (Fig. 2M). This lack of septum cell degradation was still visible at late stages of fruit development: at stages 17-18 the integrity of septum cells was still maintained (Fig. 2N,O). Also, the imperfect septum fusion was still visible (Fig. 2O), which probably corresponds to the division line observed in Fig. 2G.

The third phenotype that we noticed was the alteration in septum thickness. In wild-type, *ntt*, and *stk* single mutant gynoecia at anthesis (stage 13), septum thickness is around six to seven cells ($n=5$). At this stage, septa from *ntt stk* double mutant gynoecia presented no difference in the number of cells. Note, however, that pollen tube growth is affected in *ntt stk* gynoecia, as discussed in the next paragraph (Fig. S2). However, at stage 17-18, septa thickness in

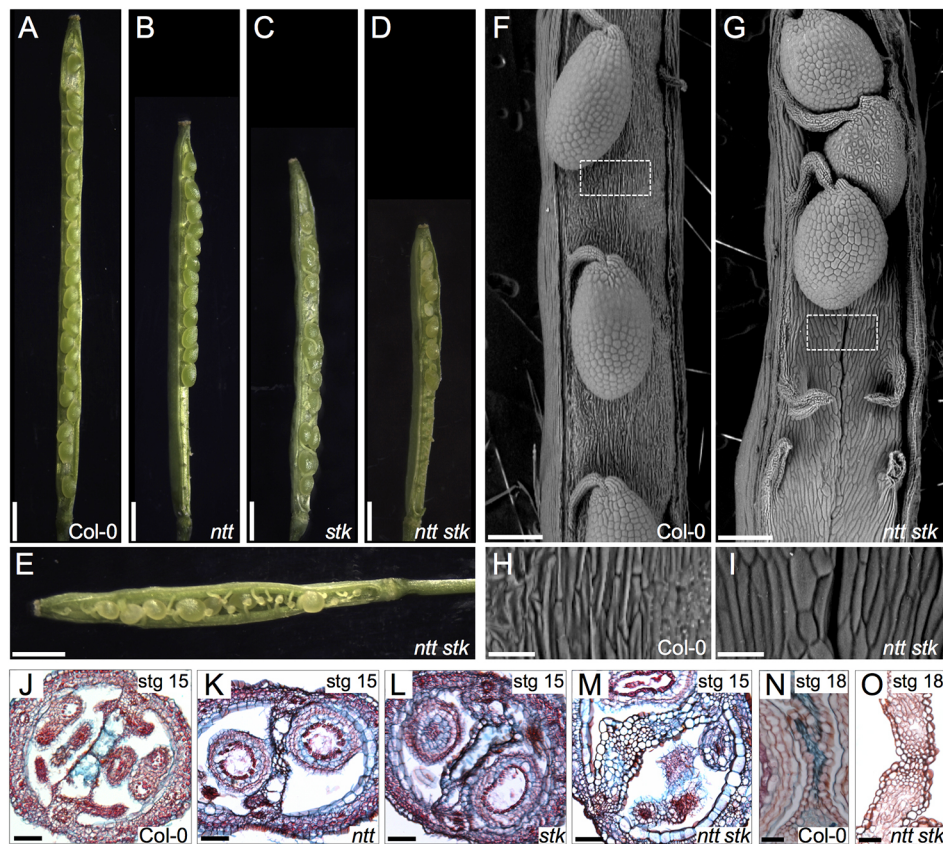


Fig. 2. The *ntt stk* double mutant is affected in gynoecium medial domain development. (A-E) Images of Col-0 (A), *ntt* (B), *stk* (C) and *ntt stk* (D,E) fruits, showing affected seed-set and septum development. (F-I) Scanning electron microscopy images of Col-0 (F,H), and *ntt stk* (G,I) fruits and septum. H and I are magnifications of the boxed areas in F and G, respectively. (J-O) Alcian Blue- and Neutral Red-stained transverse sections of Col-0 (J), *ntt* (K), *stk* (L) and *ntt stk* (M) stage 15 fruits, and Col-0 (N) and *ntt stk* (O) stage 17 septa. Scale bars: 1 mm in A-E; 200 μ m in F,G; 50 μ m in H-M; 25 μ m in N,O.

ntt stk fruits increased to ten cells (Fig. 2O). In summary, these results suggest that the simultaneous loss of NTT and STK activity leads to altered septum fusion and delays entry of septum cells to their normal degradation program.

Pollen tube growth and seed-set are affected in the *ntt stk* double mutant

The observed septum defects in the *ntt stk* double mutant could account for the reduced seed-set and fruit length (Fig. 3). Reduction in seed-set and fruit length has previously been observed for the *ntt* single mutant (Crawford et al., 2007). For the *stk* single mutant, a reduction in fruit length has been reported (Pinyopich et al., 2003) as well as a slight reduction in seed-set (Mizzotti et al., 2012). The transmitting tract differentiates at stage 12 and it is functional at the mature gynoecium stage when anthesis occurs (stage 13). In the *ntt* mutant, no transmitting tract is formed (Fig. 2K) and seed-set is only observed in the apical part of the fruit, owing to reduced pollen tube growth (Crawford et al., 2007). In the *stk* mutant, Alcian Blue staining of gynoecia suggests that transmitting tract formation is not affected, and the pattern of seed-distribution is similar to wild type (Fig. 2C,L; Fig. S2).

We tested whether the absence of transmitting tract and the absence of dead cells in the septum caused by the *ntt stk* double mutation could further affect pollen tube growth through the ovary. Therefore, we monitored pollen tube movement in *ntt stk* gynoecia using Aniline Blue staining. As expected, we observed pollen tubes that reached the ovules along the wild-type and *stk* ovaries (Fig. 3C,E). By contrast, as reported before, in the *ntt* mutant, pollen tube growth was mainly observed in the apical part of the ovary (40-50% of total ovary length; Fig. 3D). In the *ntt stk* double mutant, pollen tube growth was further affected, and observed only in the upper 20% of total ovary length (Fig. 3F).

Our results suggest that NTT and STK together impact cell degradation in the septum and, as a consequence, affect the transmitting tract, fertilization efficiency and final seed-set.

A co-expression network links *NTT* and *STK* to their putative transcriptional targets

To gain further insight into the biological processes controlled by NTT and STK, we generated an ARACNE-based co-expression network of flowers for both transcription factors (see Materials and Methods). Connections in this network indicate transcriptional correlation between genes. Three gene groups could be identified: those connected to *NTT*, those connected to *STK*, and those genes connected to both *NTT* and *STK*. The complete list of genes in the network is presented in Table S2 and illustrated in Fig. S7. We focused on the third group (genes connected to both *NTT* and *STK*), which we called the core network (Fig. 4A). Interestingly, in the core network two transcription factors belonging to the REPRODUCTIVE MERISTEM (REM) family are present, *REM11* and *REM13*, which are known to be expressed in the developing gynoecium, specifically in the CMM and ovules (Wynn et al., 2011; Mendes et al., 2016), and the transcription factor *HAF*, known to be involved in transmitting tract development (Crawford and Yanofsky, 2011). Recently, *REM11* (also known as *VALKYRIE*) already has been shown to be a direct target of STK (Mendes et al., 2016), providing evidence that supports this co-expression network. Furthermore, in the core network four enzyme and transporter-encoding genes are present: *AT1G28710* (a nucleotide-diphospho-sugar transferase family gene), *AT3G26140* (a family 5, subfamily 11 glycosyl hydrolase), *AT3G21090* (ABC transporter G family member 15, *ABCG15*) and *AT1G06080* (δ -9 acyl-lipid desaturase 1, *ADS1*), related to polysaccharide metabolism or membrane lipid transport and synthesis (Kang et al., 2011; Li-Beisson et al., 2013).

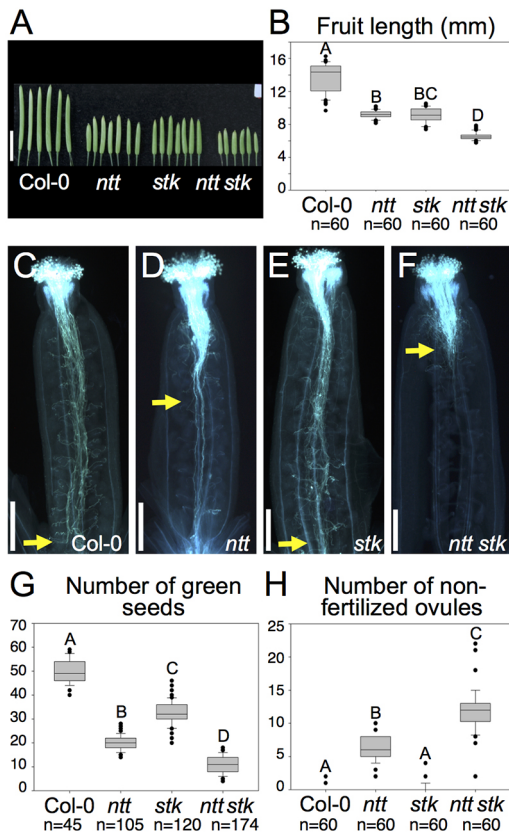


Fig. 3. Seed-set is affected in the *ntt stk* double mutant. (A,B) Overview of Col-0, *ntt*, *stk* and *ntt stk* fruits and length analysis (B). (C-F) Aniline Blue staining of Col-0 (C), *ntt* (D), *stk* (E) and *ntt stk* (F) pollen tubes in stage 13 gynoecia. Pollen tubes are visible as cyan filamentous structures. Yellow arrows indicate the location up to where pollen tube growth is observed. (G,H) Green seed number (G) and non-fertilized ovules (H) in Col-0, *ntt*, *stk* and *ntt stk* fruits. Boxes indicate first quartile (Q1), median, third quartile (Q3); whiskers indicate minimum and maximum; dots represent outliers. Statistical analyses were performed using an ANOVA followed by Tukey HSD tests. Letters indicate statistically different groups ($P < 0.01$). Scale bars: 0.5 cm in A; 200 μ m in C-F.

In co-expression networks, the connection between two nodes may indicate a possible direct regulation when transcription factors are involved (Serin et al., 2016; van Dam et al., 2017). NTT and STK are both transcription factors, so they might directly regulate the expression of the core genes. A consensus binding site for NTT is not known, so we used the DNA-binding site predictor for C2H2 zinc finger proteins (Persikov and Singh, 2013). For MADS-box proteins the consensus binding site is well-known and is called the CarG-box (de Folter and Angenent, 2006). We analyzed whether putative binding sites for NTT and STK were present in promoter or intron sequences of the core network genes. Interestingly, the regulatory regions of all core network genes have putative binding sites (Fig. 4B).

NTT and STK are regulators of cell wall and lipid metabolism genes

To confirm experimentally the putative transcriptional regulation of the core network genes by NTT and STK, and to understand better the biochemical processes through which NTT and STK exert their effect in the tissues, we obtained experimental evidence for their regulation of the genes coding for enzymes and a transporter involved in cell wall polysaccharide and lipid metabolism (Fig. 4). Interestingly, recently it has been shown that STK is involved in cell

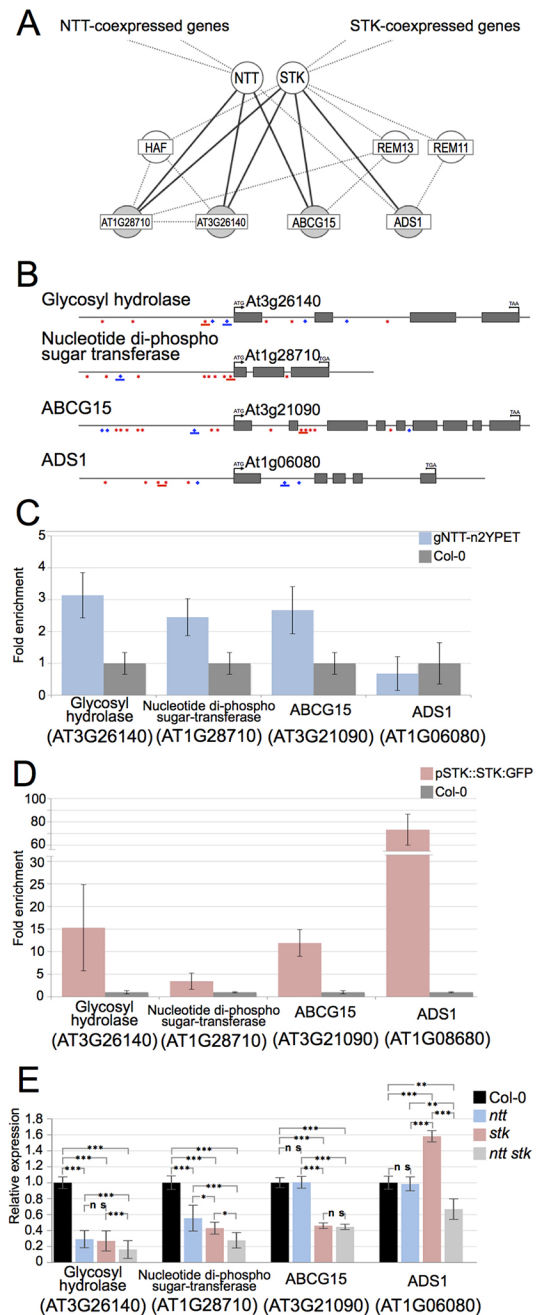


Fig. 4. NTT and STK are co-expressed with cell wall and lipid metabolism enzyme and transporter-encoding genes. (A) NTT-STK core co-expression network. Nodes represent genes and edges represent co-expression. White nodes are transcription factors and gray nodes represent enzyme- and transporter-encoding genes. Dotted lines represent co-expression and solid lines represent possible direct regulation based on ChIP experiments. (B) Schematic of the four enzyme- and transporter-encoding genes present in the core network; arrows indicate the translation start site; gray boxes represent exons; red asterisks indicate CarG-boxes and blue diamonds indicate predicted NTT-binding sites (TCWNAGS); lines under the asterisks/diamonds indicate regions selected for ChIP enrichment tests. (C) ChIP-qPCR results of regulatory regions (blue lines in B) using a *gNTT::n2YPET* line versus wild type. (D) ChIP-qPCR results of CarG-box-containing regulatory regions (red lines in B) using a *STK::STK:GFP* line versus wild type. A representative experiment is shown. Error bars represent the s.d. of three technical replicates. (E) qRT-PCR results of the enzyme-coding genes present in the core network in Col-0, *ntt*, *stk* and *ntt stk* gynoecia. Error bars represent the s.d. of three biological replicates. Statistical analyses were performed using a Tukey test: * $P < 0.05$, ** $P < 0.01$, *** $P < 0.001$. n.s., not significant.

wall architecture of the seed (Ezquer et al., 2016). First, we performed chromatin immunoprecipitation (ChIP) assays using an anti-GFP antibody on wild-type, *STK::STK::GFP* and *gNTT-n2YPET* inflorescence tissue, followed by qPCR analysis (Fig. 4C,D). Compared with wild type, ChIP-qPCR results from the *STK::STK::GFP* line showed a significant enrichment of promoter/intron regions for all four genes tested (Fig. 4D). ChIP-qPCR results from the *gNTT-n2YPET* line showed a significant enrichment of promoter regions for three genes (Fig. 4C). No enrichment was observed for *ADSI*, although we cannot exclude the possibility of NTT binding to other sites.

We then reasoned that if NTT and/or STK are transcriptional regulators of the genes present in the core network their expression should be altered in the *ntt*, *stk* and *ntt stk* mutant backgrounds. We analyzed the expression of the four enzyme- and transporter-encoding genes present in the core co-expression network using qRT-PCR (Fig. 4E). The expression of all four genes was reduced in the *ntt stk* double mutant gynoecia, compared with the wild-type sample (Fig. 4B). The *AT3G26140* and *AT1G28710* genes presented a roughly similar reduction in expression levels in the single and double mutants, which suggests that these genes could be under the control of an NTT- and STK-containing protein complex, such that single disruption of *NTT* or *STK* is enough to impact the regulatory effect of the complex. Note that we could still detect some expression in the double mutant, suggesting they are regulated by more genes. On the other hand, we could not detect a difference

in expression level of *ABCG15* and *ADSI* in whole inflorescence tissue tested in the *ntt* single mutant background. Furthermore, *ADSI* expression was slightly increased in the *stk* single mutant. Nevertheless, ChIP and expression analyses support a role for NTT and STK as regulators of the genes present in the core co-expression network.

One of the genes present in the core network, *AT3G26140*, encodes a glycosyl hydrolase (GH5_11). The GH5 *Arabidopsis* enzymes that have been biochemically characterized are all mannan endo-beta-1,4-mannosidases (mannanase; E.C. 3.2.1.78), which are involved in cell wall remodeling. Although no biochemical evidence is available for GH5_11 enzymes (Aspeborg et al., 2012), it is possible that *AT3G26140* could also encode a mannanase involved in septum development, in particular the deposition or remodeling of the transmitting tract polysaccharide matrix. We therefore decided to explore further the role of *AT3G26140* in developing gynoecia. For this, we performed *in situ* hybridization for *AT3G26140* in wild-type, *ntt*, *stk* and *ntt stk* genetic backgrounds (Fig. 5A-H; Fig. S4). In wild-type gynoecia, signal was detected from early developmental stages in the CMM, in septa, funiculi and ovules (Fig. 5A,E). In the *ntt* and *stk* single mutants, comparable expression patterns were observed (Fig. 5B,C, F,G), although this is not reflected by the qRT-PCR results on whole inflorescence tissue, suggesting that there is tissue-dependent regulation. However, and in accordance to the qRT-PCR results, in the *ntt stk* double mutant only a weak signal was detected

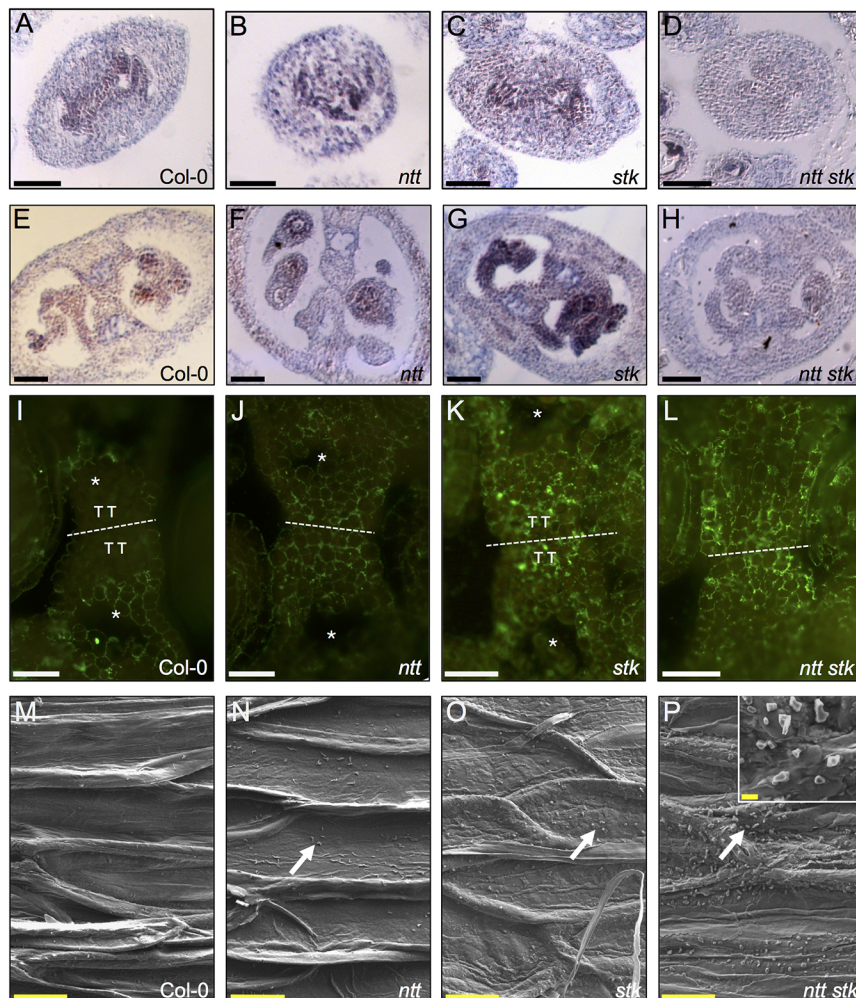


Fig. 5. NTT and STK control polysaccharide distribution and lipid metabolism in septum cells. (A-H) *In situ* hybridization of *AT3G26140* mRNA in Col-0 (A,E), *ntt* (B,F), *stk* (C,G) and *ntt stk* (D,H) in stage 8-9 (A-D) and stage 12 (E-H) gynoecia. (I-L) Immunolabeling of mannan polysaccharides in Col-0 (I), *ntt* (J), *stk* (K) and *ntt stk* (L) septa of stage 12 gynoecia; the septum fusion zone is indicated with a white dashed line; TT indicates the transmitting tract (only present in wild type and *stk*); asterisks indicate cell degradation zones. (M-P) SEM images showing wax deposition on the septum epidermis of mature fruits of Col-0 (M), *ntt* (N), *stk* (O) and *ntt stk* (P); the inset in P shows a 10,000 \times magnification of wax granules; arrows indicate wax deposition. Scale bars: 50 μ m in A-H; 20 μ m in I-L; 10 μ m in M-P; 1 μ m in P, inset.

(Fig. 5D,H). This indicates that *AT3G26140* is regulated by NTT and STK and suggests that this enzyme participates in cell wall metabolism in the cells of medial domain tissues.

Mannan and lipid deposition are altered in *ntt stk* septum cells

We observed a low *AT3G26140* mRNA signal by *in situ* hybridization in gynoecia of the *ntt stk* double mutant (Fig. 5), and we wondered if this could be translated into an altered mannan content in septum cell walls. We analyzed mannan polysaccharides distribution in septum cells during gynoecium development by immunofluorescence using the LM21 antibody, which recognizes mannan, glucomannan and galactomannan polysaccharides (Marcus et al., 2010). Significant labeling was detected in septum cell walls, but almost no signal was detected in cells of the transmitting tract of wild-type gynoecia (Fig. 5I). In the *ntt* mutant, which lacks transmitting tract tissue, a low but detectable mannan signal was present throughout the septum, as expected (Fig. 5J). Surprisingly, in the *stk* single mutant signal was detected in the septum, but also in the transmitting tract tissue, suggesting that transmitting tract cells in the *stk* mutant have an altered cell wall polysaccharide composition (Fig. 5K). In the *ntt stk* double mutant, which as in the *ntt* mutant also lacks transmitting tract tissue, a continuous signal was observed throughout the gynoecium (Fig. 5L). These results suggest that NTT and STK are both necessary for the correct expression of the putative mannanase-encoding gene *AT3G26140* in the medial domain.

The presence of lipid-related genes in the core co-expression network also prompted us to look for possible lipid deposition

defects in *ntt stk* septum cells. Using SEM we observed the presence of wax granules on the septum epidermis cells of mature (stage 19-20) fruits (Fig. 5M-P). These wax granules were scarce on wild-type septum cells, but clearly visible in the *ntt* or *stk* single mutants (Fig. 5N,O, arrows). In the *ntt stk* double mutant a larger number of wax granules was observed (Fig. 5P).

Mutations in *ABCG15* (*KAWAK*) severely affect gynoecium development

In order to study the individual contribution of the enzyme and transporter-encoding genes to the *ntt stk* phenotype, we analyzed T-DNA insertion lines for two NTT-STK target genes (Fig. 4). For the putative mannanase-encoding gene *AT3G26140*, a statistically significant reduction in seed-set and fruit length was detected (Fig. S5). The mild phenotype could be explained by functional redundancy among cell wall regulators.

For *ABCG15*, we obtained two mutant alleles that showed dramatic and pleiotropic phenotypes, probably related to altered meristematic activity (Fig. 6; Fig. S6). We named this transporter *KAWAK* (*KWK*), which comes from Mayan mythology. It is the name of one of the 20 months of the Mayan calendar, and it means ‘storm’ and also ‘monster with two heads’. In these *kwk* mutant plants, shoot apical meristem (SAM) maintenance was reduced or even absent (Fig. 6A; Fig. S6). The loss of the apical dominance caused growth of secondary shoots. Defects were also observed in inflorescence and floral meristems, causing altered floral bud positioning and number, and alterations in floral organ arrangement (Fig. 6; Fig. S6). Furthermore, we observed floral organ fusion defects, unfused carpels and septa, ectopic formation of ovules and

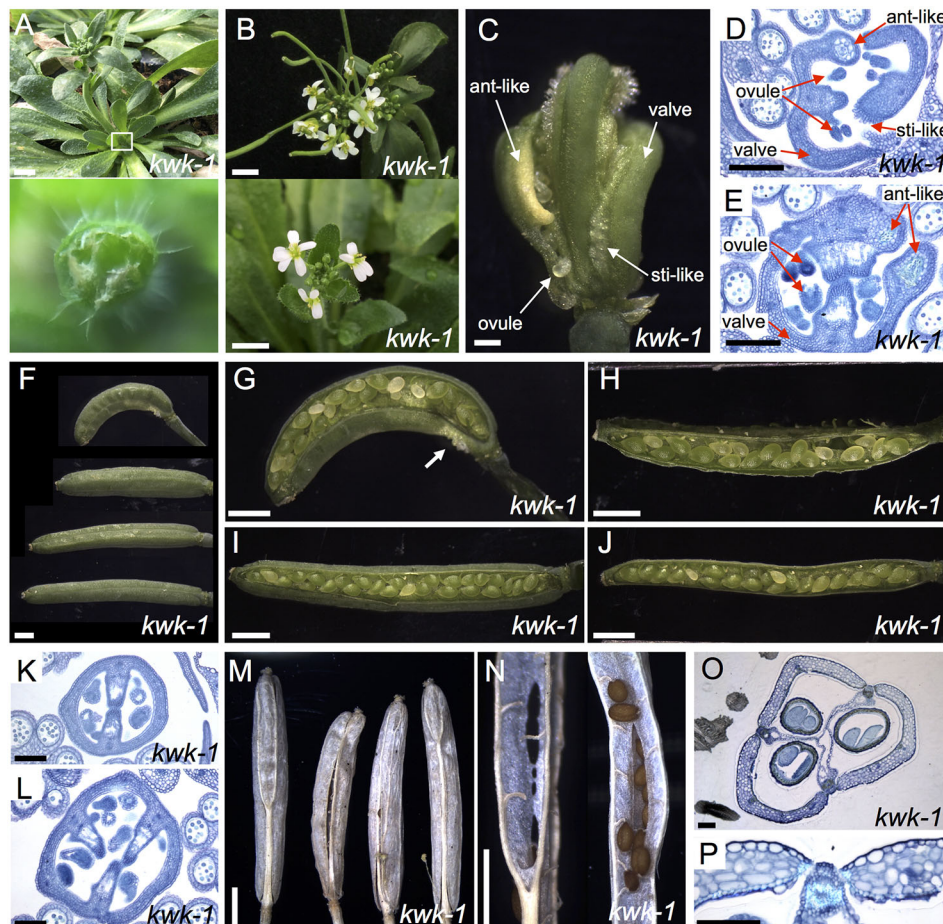


Fig. 6. The *kwk* mutant is affected in meristematic activity and reproduction. (A) Defects in SAM maintenance can lead to meristem arrest and loss of apical dominance (lower panel is a magnification of the boxed area in A). (B) Inflorescences with abnormal phyllotaxis and flowers with defects in organ number. (C) Gynoecium with fusion defects and growth abnormalities. (D,E) Transverse sections of Toluidine Blue-stained gynoecia; anther-like (ant-like) or stigma-like (sti-like) tissues are visible. (F) Overview of the shape of *kwk-1* fruits. (G-J) Internal view of fruits showing defects in seed formation and septum fusion. (K,L) Transverse sections of fruits with two or three valves. (M,N) External (M) and internal (N) views of mature fruits. (O) Transverse section of a mature fruit with three valves. (P) Toluidine Blue staining reveals that fruit lignification and dehiscence is normal in *kwk-1*. Scale bars: 5 mm in A,B; 200 μ m in C; 100 μ m in D,E,K,L,O,P; 2 mm in F-J,M,N.

stigmatic tissue or repla. Fruits developed from less-affected gynoecia presented alterations in carpel number, and all fruits had alterations in seed formation and seed arrangement, the latter probably due to funiculi alterations (Fig. 6F-P; Fig. S6). These results highlight the importance of ABCG15 (KAWAK) during *Arabidopsis* development, making it an interesting target of NTT and STK to study further in future work.

DISCUSSION

Multiple roles have been reported for the NTT transcription factor during gynoecium development, including transmitting tract formation (Crawford et al., 2007), replum development (Marsch-Martínez et al., 2014) and valve margin specification (Chung et al., 2013). We identified that NTT interacts with a large number of transcription factors belonging to different families, suggesting that NTT participates in many protein complexes during development, possibly performing different, as yet unknown, functions.

In this work, we focused on the interaction with STK, a MADS-box protein that determines ovule identity, correct funiculus development, seed abscission (Pinyopich et al., 2003; Balanzà et al., 2016) and regulation of seed development (Mizzotti et al., 2014; Ezquer et al., 2016). MADS-box transcription factors are able to interact with each other and form functional protein complexes that guide flower development (Honma and Goto, 2001; de Folter et al., 2005; Immink et al., 2009). For STK, protein-interaction partners important for ovule and seed development, such as AG, SEPALLATA3 (SEP3) and ARABIDOPSIS B SISTER (ABS), have been reported (de Folter et al., 2005; Kaufmann et al., 2005; de Folter et al., 2006; Mizzotti et al., 2012). In general, MADS-box proteins interact with MADS family members, and few interactions with members of other transcription factor families have been described to date (Smaczniak et al., 2012; Bemer et al., 2017). Interestingly, we found that NTT, a zinc finger transcription factor, interacts with various MADS-box proteins such as AG, SHP1, SHP2 and STK, which are all paralogs (Marsch-Martínez et al., 2014; this work). Based on the data presented in this work, we suggest that NTT and STK can work cooperatively during gynoecial medial domain development in *Arabidopsis*.

Co-expression network to identify target genes

One of the current challenges in understanding the regulation of flower development is the identification of transcriptional targets of key transcription factors (Wellmer et al., 2014). In order to identify possible target genes of NTT and STK, we generated an ARACNE-based co-expression network, which uses microarray expression data and infers putative transcriptional interactions (Margolin et al., 2006a) (Fig. 4A). Networks inferred using this method are a useful tool in the understanding of biological processes (Yu et al., 2011; Chávez Montes et al., 2014; González-Morales et al., 2016).

Interestingly, by searching in the current literature, we found that many of the inferred interactions in the NTT-STK co-expression network are supported by several reports, indicating that these interactions are biologically relevant. There are examples of functional interactions between STK and SHP2 (Pinyopich et al., 2003; Brambilla et al., 2007) and, in some cases, of direct transcriptional regulation, for instance STK to *VERDANDI* (Matias-Hernandez et al., 2010), *BANYULS* (Mizzotti et al., 2014), and *REM11* (Mendes et al., 2016). These genes are present in the NTT-STK co-expression network (Table S1). For NTT, a transcriptional relationship with *HAF* has been reported (Crawford and Yanofsky, 2011), which is also connected in the network to STK. Besides *HAF*, *REM11* and *REM13* are also connected to NTT and STK in the

network, and they are expressed in young gynoecia in the CMM (Wynn et al., 2011; Mantegazza et al., 2014), which supports a role for NTT and STK in early gynoecium development. Beyond transcription factors, four enzyme and transporter-encoding genes are co-expressed with NTT and STK (Fig. 4). These enzymes and transporter could provide clues about the biochemical processes regulated by NTT and STK.

ChIP experiments indicated binding of STK to CArG-box-containing regions in the promoters/introns of all four genes, and binding of NTT to putative C2H2 zinc finger protein-binding sites of at least three genes, suggesting that they could be direct STK/NTT targets. Moreover, qRT-PCR experiments showed reduced expression of all four enzyme-encoding genes in the *ntt stk* double mutant; however, this was not the case for all of the single mutants, possibly due to redundancy. But, in general, the results suggest that these enzyme- and transporter-encoding genes are targeted by NTT and/or STK (Fig. 4).

The first enzyme (AT3G26140) we found belongs to the GH5 family for which (1-4)-beta-mannan endohydrolase and cellulase activities have been identified for some members (Aspeborg et al., 2012). The second enzyme is a nucleotide-diphospho-sugar transferase (AT1G28710), a glycosyltransferase involved in the synthesis of polysaccharides. Based on the CAZy database, it belongs to the GT77 family for which α -xylosyltransferase (EC 2.4.2.39), α -1,3-galactosyltransferase (EC 2.4.1.37) and arabinosyltransferase (EC 2.4.2.-) activities have been reported (Lombard et al., 2014). The third enzyme, ADS1 (AT1G06080), has been characterized as a functional fatty acid desaturase (Yao et al., 2003; Heilmann et al., 2004) and is expressed in flowers (Fukuchi-Mizutani et al., 1998). Heterologous expression of this enzyme in *Brassica juncea* generated decreased levels of total saturated fatty acid in seeds and altered the normal fatty acid profile (Yao et al., 2003). The last gene is ABCG15 (AT3G21090), an ATP-binding cassette (ABC) transporter, which we named KAWAK (KWK; discussed below). Members of this ABCG group are required for lipid deposition and cutin formation (Kang et al., 2011). ABCG15 is phylogenetically close to ABCG12 (also known as CER5), which is required for wax transport to the cuticle (Pighin et al., 2004), and it is also close to ABCG13, which is involved in the transport of cuticular lipids in flowers (Panikashvili et al., 2011), and to ABCG11 (also known as DSO), which is involved in cuticular lipid export (Bird et al., 2007; Luo et al., 2007; Panikashvili et al., 2007; Ukitsu et al., 2007).

So, the four genes found are related to cell wall polysaccharide metabolism or membrane lipid synthesis and transport. Our findings suggest that these two processes are altered in septum cells of the *ntt stk* mutant. We have recently shown that global changes in cell wall composition take place during gynoecium development (Herrera-Ubaldo and de Folter, 2018), for instance mannan polysaccharide content decreases when the gynoecium matures. Here, mannan polysaccharide content in mutant and wild-type gynoecia was analyzed; an evident alteration in mannan accumulation was observed in the medial region of the single and double mutants, suggesting that the reduction in expression of the mannanase gene *AT3G26140* observed by *in situ* hybridization and qRT-PCR could be related to the increase in mannan accumulation. Reduced fertility is to be expected when this enzyme is affected, which we did indeed observe in a T-DNA insertional mutant for *AT3G26140* (Fig. S5). The subtle reduction in fertility observed is probably due to the involvement of other redundant proteins or additional enzymes. This was recently shown for silique dehiscence zone formation, where various cell wall-modifying enzymes participate, such as

ARABIDOPSIS DEHISCENCE ZONE POLYGARACTURONASE 1 (ADPG1), ADPG2, CELLULASE 6 (CEL6) and MANNANASE 7 (MAN7) (Ogawa et al., 2009; He et al., 2018). On the other hand, the altered wax deposition in septum cells is a sign of altered lipid metabolism or transport. Alterations in these processes could explain the phenotypes observed in the *ntt stk* double mutant.

Septum fusion and cuticle formation

Defects in septum fusion were observed in the *ntt stk* double mutant. However, these defects are different to those observed in, for example, the *spt* mutant, which has a reduced cell number in the CMM and reduced growth of the septa primordia (Alvarez and Smyth, 1999, 2002; Heisler et al., 2001). Cell number in the CMM in the *ntt stk* mutant is similar to that observed in wild type, and septa primordia grow normally and encounter each other to form the septum. This suggests that the observed fusion abnormalities (Fig. 2) are not related to defects in early growth, but might be related to epidermal defects, such as altered cuticle, which is a specialized lipidic modification of the cell wall (Yeats and Rose, 2013). Cuticle seems to be involved in cell-to-cell communication (Tanaka and Machida, 2007), and alterations in cuticle formation cause organ fusion defects (Nawrath, 2006).

The correct formation and composition of the cuticle is important for flower development, as it promotes carpel fusions and prevents ectopic or organ fusions (Lolle and Cheung, 1993; Panikashvili et al., 2010). Mutants such as *fiddlehead* and *hothead* have floral organ fusion defects caused by altered cuticle formation (Lolle et al., 1998; Yephremov et al., 1999; Pruitt et al., 2000; Krolkowski et al., 2003). Interestingly, a mutation in the epidermis-expressed ABCG11 transporter (related to ABCG15) affects organ fusion due to altered epicuticular wax on the surface of organs (Luo et al., 2007; Panikashvili et al., 2010). We also observed altered wax deposition on the septum surface of the *ntt stk* double mutant, which could be related to its septum fusion defects. Furthermore, the expression of *ABCG15* was clearly reduced in the double mutant and regulatory regions of *ABCG15* were enriched in ChIP assays for STK and NTT (Fig. 4). Interestingly, we identified *kwk* mutants that showed dramatic phenotypes in meristem development and during reproductive development. Alterations in the ABCG15 transporter function could lead to impaired lipid export and altered cuticle formation. It could also affect membrane structure or block the correct position of membrane proteins. The *kwk* mutant might be helpful in understanding the role of plant surface lipids and epidermis development, and the role of the epidermis in developmental processes (e.g. Delude et al., 2016; Verger et al., 2018).

Cell integrity and senescence

Modifications of the cell wall and cell death are important processes during the formation of the transmitting tract and its ECM that allow for pollen tube growth through the ovary, and therefore directly affect fertilization efficiency and seed-set (Crawford et al., 2007; Crawford and Yanofsky, 2008). The *ntt* mutant lacks a transmitting tract, as indicated by the lack of acidic polysaccharide staining. However, cell degradation does take place in the septum, observed as irregular-shaped, degraded cells and empty spaces (Crawford et al., 2007; Fig. 2). These tissues appear normal in the *stk* mutant. The *ntt stk* double mutant, however, lacks cell degradation in the septum. Moreover, the double mutation produces a clear increase in severity of pollen tube growth through the gynoecium. Whereas pollen tube growth is reduced in the single *ntt* mutant, and does not appear to be affected in the *stk* mutant, it is severely reduced in the *ntt stk* double mutant.

Part of the altered cell degradation phenotype could be related to the observed lack of mannanase expression in the medial domain of young *ntt stk* gynoecia. Furthermore, the nucleotide-diphospho-sugar transferase might be involved in the synthesis of any of the polysaccharides, glycoproteins or glycolipids of the ECM, suggested to provide nutrients and adhesion for correct pollen tube growth (Crawford and Yanofsky, 2008).

Taken together, the data presented indicate that NTT and STK have clear roles in septum fusion and the modification of cell walls, affecting fertilization efficiency and seed-set.

Another important process for which cell wall modifications play a role is during fruit ripening, which is followed by senescence (Gapper et al., 2013; Gómez et al., 2014). Our work also hints that senescence is induced by NTT and STK (Fig. S1). Note that we observed already some induced senescence and cell death by NTT alone, and this could be due to interactions with other proteins, possibly with other related MADS-box proteins (Fig. S3). Though arguably a bit preliminary, this suggests that NTT, enhanced by STK, can promote senescence and induce cell death and, thereby, might regulate fruit maturation. Research in tomato has demonstrated that MADS-box proteins control fruit ripening (Karlova et al., 2014). *RIPENING INHIBITOR (RIN)*, a homolog of the *Arabidopsis* SEP genes (Vrebalov et al., 2002), regulates the expression of genes involved in cell wall modifications, such as polygalacturonase and B-galactosidase, in addition to proteins controlling shelf life (A-expansin) and fruit softening (B-mannanase) (Fujisawa et al., 2011). The latter is dramatically downregulated in fruit ripening-defective tomato plants (Fujisawa et al., 2014; Shima et al., 2014). Other MADS-box genes involved in tomato fruit ripening are homologs of the *AG* clade (Itkin et al., 2009; Vrebalov et al., 2009; Pan et al., 2010) and *FUL* homologs (Bemer et al., 2012). In addition, some zinc finger proteins are also involved in fruit ripening, such as SIZFP2 (Rohrmann et al., 2011; Weng et al., 2015) and MaC2H2-1/2 (Han et al., 2016).

In summary, we found that NTT and STK control genes coding for enzymes and transporters involved in synthesis and degradation of cell wall polysaccharides, and synthesis and transport of fatty acids. It would be particularly interesting to know whether homologous genes could perform similar activities in other fruits, especially those important for food and industry.

MATERIALS AND METHODS

Plant material and growth

Arabidopsis thaliana plants were germinated in soil (3:1:1, peat moss: perlite:vermiculite) in a growth chamber under long-day conditions (16 h light, 22°C; 8 h dark, 20°C) for 10 days and transferred to standard greenhouse conditions (22–27°C, natural light). The following mutants and lines were used in this work: the transposon insertion line *ntt-3* is the NASC line N104422 (SM_3.16705) in Col (Tissier et al., 1999); *stk-2* (Pinyopich et al., 2003); *STK::GUS* (Kooiker et al., 2005); *35S::STK* (Favaro et al., 2003); *35S::NTT* (Marsch-Martínez et al., 2014); *gNTT-n2YPET* (Crawford et al., 2015); *kwk-1* is the line GT_5_99063 in *Ler* (T-DNA in the third exon); *kwk-2* is SALKseq_125172 in Col-0 (T-DNA in the third exon); insertion line for *AT3G26140* is SALK_128093 (T-DNA in the third intron); *Nicotiana benthamiana* and *Nicotiana tabacum* were used for cell death assays and BiFC, respectively.

NTT::GUS construct

For the NTT promoter::GUS fusion, a 1216 bp DNA sequence upstream of the predicted translation start was amplified by PCR from genomic Col-0 DNA, using Pwo DNA polymerase (Roche) and primers S314 and S318 (Table S3). The PCR product was cloned in front of the GUS ORF of the binary vector pANGUS [a derivative of pPAM (GenBank AY027531) described by Stracke et al., 2007] using the restriction endonucleases

Clal and *NcoI*. *A. thaliana* Col-0 was transformed by floral dip (Clough and Bent, 1998).

Y2H assay

Y2H assays were performed using the GAL4 system (pDEST22 and pDEST32; Invitrogen) as previously described (de Folter et al., 2005; de Folter and Immink, 2011). NTT-BD cloning and yeast autoactivation test was previously described (Marsch-Martínez et al., 2014). The STK-AD clone was derived from recombining the *STK* Gateway ENTRY clone from the EU-REGIA project (Paz-Ares and The REGIA Consortium, 2002) with the pDEST22 vector (Castrillo et al., 2011). We used the yeast strain PJ69-4 mating type A and α (James et al., 1996). The uni-directional Y2H screen with 45 selected AD clones has been described before (Zúñiga-Mayo et al., 2012; Marsch-Martínez et al., 2014; Lozano-Sotomayor et al., 2016), but, in short, it contains selected transcription factors from the EU-REGIA project (Paz-Ares and The REGIA Consortium, 2002) that are known to be involved in flower and gynoecium development, and meristem activity (Table S1). Interaction assays were performed on SD-GLUC medium lacking Leu, Trp and Ade, and on medium lacking Leu, Trp and His, supplemented with 20 mM 3-AT. Protein-protein interactions were scored after 5 days of growth at 25°C. Positive results (yeast growth) were confirmed by a *lacZ* assay.

BiFC assay

In planta protein interaction assays were performed as previously described (Marsch-Martínez et al., 2014). The cDNA of *STK* was cloned in pDONR201 (Invitrogen) by the REGIA Consortium (Paz-Ares and The REGIA Consortium, 2002). This clone was recombined with pYFN43 (Belda-Palazón et al., 2012) using an LR Gateway-based reaction to generate N-terminal fusions with the N-terminal part of YFP. NTT entry clone was also recombined with pYFC43 (Belda-Palazón et al., 2012) to generate an N-terminal fusion with the C-terminal part of the YFP protein. The constructs were individually introduced in to *Agrobacterium tumefaciens* GV2260 and cultured on LB supplemented with 100 µg/ml kanamycin and 25 µg/ml rifampicin. Overnight cultures of *Agrobacterium* (O.D.: 1.2-1.6) were collected and re-suspended in a similar volume of infiltration medium (10 mM MgCl₂, 10 mM MES pH 5.6, 200 µM acetosyringone), the O.D. was adjusted to 1.0, and the re-suspension was incubated at 25°C during 3 h with weak shaking. Before co-infiltration, *Agrobacterium* containing pYFC43-NTT was mixed with a similar volume of *Agrobacterium* with pYFN43-STK. This mixture was introduced in the abaxial air space of young *Nicotiana tabacum* leaves using a needle-less syringe. YFP fluorescence restoration was assayed 2 days after infiltration using an inverted LSM 510 META confocal laser scanning microscope (Carl Zeiss). YFP was excited using the 488 nm line of an argon laser and emission was filtered using a BP 500-550 nm filter.

Histology and microscopy analyses

For thin tissue section analysis, inflorescences and stage 15, 17-18 fruits of Col-0, *ntt-3*, *stk-2*, and *ntt stk* were collected (according to Smyth et al., 1990), tissue was fixed in FAE solution (3.7% formaldehyde, 5% glacial acetic acid and 50% ethanol) with vacuum (15 min, 4°C) and incubated for 60 min at room temperature. The material was rinsed with 70% ethanol and incubated overnight at 4°C in 70% ethanol, followed by dehydration in a series of ethanol dilutions (70%, 85%, 95% and 100% ethanol) for 60 min each. Inflorescences and stage 17-18 fruits were embedded in Technovit 7100 (Heraeus Kulzer) according to the manufacturer's instructions. Stage 15 fruits were embedded in Paraplast (Sigma-Aldrich) as previously described (Zúñiga-Mayo et al., 2012). Sections (12-15 µm) were obtained on a rotary microtome (Reichert-Jung 2040; Leica). Tissue sections were stained with a solution of 0.5% Alcian Blue and counterstained with 0.5% Neutral Red as previously described (Zúñiga-Mayo et al., 2012), or with Toluidine Blue as previously described (Herrera-Ubaldo and de Folter, 2018). *NTT::GUS* and *STK::GUS* inflorescences were collected and stained as previously described (Marsch-Martínez et al., 2014). The GUS-stained inflorescences were fixed, dehydrated as described above and embedded in Technovit 7100; 12-15 µm sections were analyzed. Pictures were taken using a DM6000B microscope (Leica).

For septum epidermis cell observations, fresh fruit samples were dissected and visualized in an EVO 40 scanning electron microscope (Carl Zeiss), using the VPSE G3 detector, with a 15-20 kV beam and at 50 Pa pressure.

Pollen tube growth within the pistil was monitored with Aniline Blue staining. Pistils were collected 24 h after pollination, and tissue fixation and softening were performed as previously described (Jiang et al., 2005). Pistils were washed with distilled water three times and stained with aniline blue solution (0.01% Aniline Blue in 150 mM K₂HPO₄ buffer, pH 11) for 4 h in the dark. Pistils were observed and imaged with a DM6000B fluorescence microscope under UV light (Leica).

Gene co-expression analysis

A flower co-expression matrix was obtained from microarray data using the ARACNE algorithm (Margolin et al., 2006a,b). Sample data relationship files for ATH1-121501 microarray experiments were downloaded in August 2016 from the ArrayExpress website (<http://www.ebi.ac.uk/arrayexpress/>; accession numbers E-GEOD-15555, E-GEOD-16056, E-GEOD-2473, E-GEOD-27281, E-GEOD-2848, E-GEOD-30492, E-GEOD-3056, E-GEOD-32193, E-GEOD-40998, E-GEOD-42403, E-GEOD-42841, E-GEOD-46050, E-GEOD-52067, E-GEOD-5526, E-GEOD-55431, E-GEOD-55799, E-GEOD-5632, E-GEOD-66419, E-MEXP-1246, E-MEXP-1592, E-MEXP-1920, E-MEXP-3293, E-MEXP-849 and E-TABM-17) and manually curated to identify 24 experiments that contained 106 high-quality microarray hybridizations for wild-type flower samples. The corresponding CEL files were manually curated and processed as previously described (Chávez Montes et al., 2014; González-Morales et al., 2016), with a single modification: custom CDF version 20 files (http://brainarray.mbni.med.umich.edu/Brainarray/Database/CustomCDF/genomic_curated_CDF.asp; Dai et al., 2005) were used for gcma normalization. The output of the ARACNE algorithm, which is a mutual information-ranked list of pairs of interactors (i.e. of co-expressed genes), was used to identify genes (both transcription factors and non-transcription factors) co-expressed with *NTT* and *STK*.

ChIP and qPCR

Genomic regions located between the flanking genes in the co-expression network core were analyzed bioinformatically to identify putative CARG-box regions and predicted NTT-binding sites (Persikov and Singh, 2014). ChIP assays were performed as previously described (Ezquer et al., 2016). One gram of unfertilized flowers from Col-0, *STK::STK::GFP* (Mizzotti et al., 2014) and *gNTT-n2YPET* (Crawford et al., 2015) plants were collected. For the immunoprecipitation, we used 2 µl anti-GFP polyclonal antibody per sample (Clontech 632460 for ChIP with STK; Roche 11814460001 for ChIP with NTT). Enrichment of the target regions was calculated by qPCR (iQ_SYBR Green Supermix, Bio-Rad) using a Bio-Rad iCycler iQ optical system. The relative enrichment of the listed targets obtained from *STK::STK::GFP* and *pNTT-n2YPET* unfertilized flowers were compared with the enrichment obtained from Col-0 wild-type unfertilized flowers. *ACTIN 7* was used for normalization as previously described (Matias-Hernandez et al., 2010). Primers used for ChIP analysis are listed in Table S3.

qRT-PCR analysis

For the qRT-PCR analysis, gynoecia from stage 7 to 12 were collected under a stereomicroscope (Stemi 2000, Zeiss). Three biological replicates were sampled for each genotype (Col wt, *ntt*, *stk*, *ntt stk*), each containing around 40 gynoecia. Total RNA was extracted using the Quick-RNA MicroPrep Kit (Zymo Research). The samples were treated with DNase I, included in the kit. Reverse transcription and amplification were performed using the KAPA SYBR FAST One-Step qRT-PCR Kit (Kapa Biosystems). The qPCR was performed on a StepOne thermocycler (Applied Biosystems). Target gene expression levels were normalized to *ACTIN 2*. Data were analyzed using the 2^{-ΔΔCt} method (Livak and Schmittgen, 2001). Primers used are listed in Table S3.

In situ hybridization

Inflorescences from Col-0, *ntt*, *stk* and *ntt stk* plants were collected, fixed and embedded in Paraplast as previously described (Sotelo-Silveira et al.,

2013). A DNA fragment corresponding to nucleotides 1176-1368 of the *AT3G26140* coding sequence was amplified using the AT3g26140_probe primers (Table S3) and cloned into pGEM-T easy vector (Promega). The sense and antisense RNA probes were synthesized by an *in vitro* transcription reaction using SP6 and T7 polymerase (Invitrogen), respectively. Digoxigenin-labeled RNA probes for detection and hybridization were prepared as previously described (Ambrose et al., 2000).

Mannan immunolabeling

Col-0, *ntt*, *stk* and *ntt stk* inflorescences were fixed overnight at 4°C in 3% paraformaldehyde, 1×PBS 1% pH 7.0. Samples were dehydrated in a series of ethanol dilutions (70%, 85%, 95% and 100% ethanol) and embedded in Technovit 7100 (Heraeus Kulzer) according to the manufacturer's recommendations. Thin sections (14-18 µm) were obtained on a rotary microtome (Reichert-Jung 2040, Leica). Sections were treated with 1 M KOH for 60 min to unmask the manna epitopes (Marcus et al., 2010). Sections were washed three times with wash buffer (2% BSA, 1% PBS pH 7.0) at room temperature before incubation with the LM21 anti-mannan monoclonal antibody (PlantProbes; Marcus et al., 2010) diluted 1:500 in wash buffer for 16 h at 25°C; as described previously (Herrera-Ubaldo and de Folter, 2018). Samples were washed three times with wash buffer and incubated for 4 h at 25°C with the secondary antibody DyLight 488-conjugated goat anti-rat IgM mu chain (ab98368, Abcam) diluted 1:1000 in wash buffer. Samples were washed twice with wash buffer and mounted in 50% glycerol. Photographs of immunolabeled samples were taken using a DM6000B microscope under UV light (Leica).

Nicotiana leaf cell death assay

Three-week-old *Nicotiana benthamiana* leaves were infiltrated with *Agrobacterium* cells containing vectors for the transient expression of NTT (pC1300intB-35SnosEX, AY560325; Kuijt et al., 2004; Marsch-Martínez et al., 2014) or GFP (pMOG800; Knoester et al., 1998) in infiltration medium (10 mM MgCl₂, 10 mM MES pH 5.6, 200 µM acetosyringone). Three different *Agrobacterium* concentrations were used (OD600: 0.2, 0.4 and 0.8). Cell death was monitored with a modified version of the Trypan Blue (TB) staining protocol (Mauch-Mani and Slusarenko, 1994). The TB solution contains: lactic acid:phenol:glycerol:distilled water (1:1:1:1) and Trypan Blue (T-0776, Sigma-Aldrich) in a final concentration of 0.25 mg/ml. Before staining, the TB solution was diluted in 2 volumes of 100% ethanol.

Leaf sections (2 cm diameter) were collected 1, 2 and 3 days after infiltration, boiled in diluted TB solution for 1 min. Samples were de-stained in chloral hydrate solution (8:1:2 w/v/v chloral hydrate:glycerol:water) during 1 h at 65°C, followed by overnight incubation in chloral hydrate solution at 50°C with shaking. The samples were washed with 70% ethanol, mounted in 50% glycerol. Brightfield images were acquired using an Eclipse E-600 microscope with a Digital Sight (DS-R1) (Nikon Instruments).

Acknowledgements

We thank lab members and other colleagues for discussions regarding this work. We also thank Karla L. González-Aguilera and Vincent E. Cerbantez-Bueno for lab logistics and technical support. We thank Brian Crawford for *gNTT-n2YPET* seeds and the ABRC and NASC for insertion lines.

Competing interests

The authors declare no competing or financial interests.

Author contributions

Conceptualization: H.H.-U., N.M.-M., S.d.F.; Methodology: H.H.-U., I.E., M.D.M., R.A.C.M., A.G.-F., P.B., M.S.; Validation: H.H.-U.; Formal analysis: H.H.-U.; Investigation: H.H.-U., P.L.-S., I.E., M.D.M., R.A.C.M., A.G.-F., J.P.-V., D.D.-R., P.B., M.S.; Writing - original draft: H.H.-U., S.d.F.; Writing - review & editing: C.F., L.C., N.M.-M., S.d.F.; Supervision: C.F., L.C., N.M.-M., S.d.F.; Project administration: S.d.F.; Funding acquisition: S.d.F.

Funding

This work was supported by the Mexican National Council of Science and Technology (Consejo Nacional de Ciencia y Tecnología, CONACyT); PhD fellowships 243380, 219883 and 254467 to H.H.-U., P.L.-S. and D.D.-R.,

respectively; grants CB-2012-177739, FC-2015-2/1061 and INFR-2015-253504 to S.d.F., and CB-2015-255069 to N.M.-M.). S.d.F., L.C. and C.F. acknowledge the support of the European Union H2020 Marie Skłodowska-Curie Actions RISE-2015 project ExpoSEED (grant 691109). I.E. acknowledges the International European Fellowship-METMADS project (FP7 People: Marie-Curie Actions; 302606) and the Università degli Studi di Milano (RTD-A; 2016).

Data availability

Sequence and data from the genes studied in this article can be found in the Arabidopsis Genome Initiative database under the following accession numbers: *NTT*, AT3G57670; *STK*, AT4G09960; mannanase (glycosyl hydrolase), AT3G26140; nucleotide di-phospho sugar transferase, AT1G28710; *ABCG15*, AT3G21090; *ADS1*, AT1G06080; *REM11*, AT5G60140; *REM13*, AT3G46770; *HAF*, AT1G25330; *ACTIN 7*, AT5G09810; *ACTIN 8*, AT1G49240.

Supplementary information

Supplementary information available online at <http://dev.biologists.org/lookup/doi/10.1242/dev.172395.supplemental>

References

- Alvarez, J. and Smyth, D. R. (1999). CRABS CLAW and SPATULA, two Arabidopsis genes that control carpel development in parallel with AGAMOUS. *Development* **126**, 2377-2386.
- Alvarez, J. and Smyth, D. R. (2002). Crabs claw and Spatula genes regulate growth and pattern formation during gynoecium development in Arabidopsis thaliana. *Int. J. Plant Sci.* **163**, 17-41.
- Alvarez, J. P., Goldshmidt, A., Efroni, I., Bowman, J. L. and Eshed, Y. (2009). The NGATHA distal organ development genes are essential for style specification in Arabidopsis. *Plant Cell* **21**, 1373-1393.
- Alvarez-Buylla, E. R., Benitez, M., Corvera-Poira, A., Chaos Cador, A., de Folter, S., Gamboa de Buen, A., Garay-Arroyo, A., Garcia-Ponce, B., Jaimes-Miranda, F., Perez-Ruiz, R. V. et al. (2010). Flower development. *Arabidopsis Book* **8**, e0127.
- Ambrose, B. A., Lerner, D. R., Ciceri, P., Padilla, C. M., Yanofsky, M. F. and Schmidt, R. J. (2000). Molecular and genetic analyses of the silky1 gene reveal conservation in floral organ specification between eudicots and monocots. *Mol. Cell* **5**, 569-579.
- Aspeborg, H., Coutinho, P. M., Wang, Y., Brumer, H., III and Henrissat, B. (2012). Evolution, substrate specificity and subfamily classification of glycoside hydrolase family 5 (GH5). *BMC Evol. Biol.* **12**, 186.
- Balanza, V., Roig-Villanova, I., Di Marzo, M., Masiero, S. and Colombo, L. (2016). Seed abscission and fruit dehiscence required for seed dispersal rely on similar genetic networks. *Development* **143**, 3372-3381.
- Belda-Palazón, B., Ruiz, L., Martí, E., Tárrega, S., Tiburcio, A. F., Culiñán, F., Farràs, R., Carrasco, P. and Ferrando, A. (2012). Aminopropyltransferases involved in polyamine biosynthesis localize preferentially in the nucleus of plant cells. *PLoS ONE* **7**, e46907.
- Bemer, M., Karlova, R., Ballester, A. R., Tikunov, Y. M., Bovy, A. G., Wolters-Arts, M., Rossetto, P. B., Angenent, G. C. and de Maagd, R. A. (2012). The tomato FRUITFULL homologs TDR4/FUL1 and MBP7/FUL2 regulate ethylene-independent aspects of fruit ripening. *Plant Cell* **24**, 4437-4451.
- Bemer, M., van Dijk, A. D. J., Immink, R. G. H. and Angenent, G. C. (2017). Cross-family transcription factor interactions: an additional layer of gene regulation. *Trends Plant Sci.* **22**, 66-80.
- Bird, D., Beisson, F., Brigham, A., Shin, J., Greer, S., Jetter, R., Kunst, L., Wu, X., Yephremov, A. and Samuels, L. (2007). Characterization of Arabidopsis ABCG11/WBC11, an ATP binding cassette (ABC) transporter that is required for cuticular lipid secretion. *Plant J.* **52**, 485-498.
- Bowman, J. L., Baum, S. F., Eshed, Y., Putterill, J. and Alvarez, J. (1999). Molecular genetics of gynoecium development in Arabidopsis. *Curr. Top. Dev. Biol.* **45**, 155-205.
- Brambilla, V., Battaglia, R., Colombo, M., Masiero, S., Bencivenga, S., Kater, M. M. and Colombo, L. (2007). Genetic and molecular interactions between BELL1 and MADS box factors support ovule development in Arabidopsis. *Plant Cell* **19**, 2544-2556.
- Castrillo, G., Turck, F., Leveugle, M., Lecharny, A., Carbonero, P., Coupland, G., Paz-Ares, J. and Oñate-Sánchez, L. (2011). Speeding cis-trans regulation discovery by phylogenomic analyses coupled with screenings of an arrayed library of Arabidopsis transcription factors. *PLoS ONE* **6**, e21524.
- Chávez Montes, R. A., Coello, G., González-Aguilera, K. L., Marsch-Martínez, N., de Folter, S. and Alvarez-Buylla, E. R. (2014). ARACNe-based inference, using curated microarray data, of Arabidopsis thaliana root transcriptional regulatory networks. *BMC Plant Biol.* **14**, 97.
- Chung, K. S., Lee, J. H., Lee, J. S. and Ahn, J. H. (2013). Fruit indehiscence caused by enhanced expression of NO TRANSMITTING TRACT in Arabidopsis thaliana. *Mol. Cells* **35**, 519-525.

- Clough, S. J. and Bent, A. F. (1998). Floral dip: a simplified method for *Agrobacterium*-mediated transformation of *Arabidopsis thaliana*. *Plant J.* **16**, 735-743.
- Colombo, L., Franken, J., Koetje, E., van Went, J., Dons, H. J., Angenent, G. C. and van Tunen, A. J. (1995). The petunia MADS box gene FBP11 determines ovule identity. *Plant Cell* **7**, 1859-1868.
- Crawford, B. C. W. and Yanofsky, M. F. (2008). The formation and function of the female reproductive tract in flowering plants. *Curr. Biol.* **18**, R972-R978.
- Crawford, B. C. W. and Yanofsky, M. F. (2011). HALF FILLED promotes reproductive tract development and fertilization efficiency in *Arabidopsis thaliana*. *Development* **138**, 2999-3009.
- Crawford, B. C. W., Ditta, G. and Yanofsky, M. F. (2007). The NTT gene is required for transmitting-tract development in carpels of *Arabidopsis thaliana*. *Curr. Biol.* **17**, 1101-1108.
- Crawford, B. C. W., Sewell, J., Golembeski, G., Roshan, C., Long, J. A. and Yanofsky, M. F. (2015). Genetic control of distal stem cell fate within root and embryonic meristems. *Science* **347**, 655-659.
- Dai, M., Wang, P., Boyd, A. D., Kostov, G., Athey, B., Jones, E. G., Bunney, W. E., Myers, R. M., Speed, T. P., Akil, H. et al. (2005). Evolving gene/transcript definitions significantly alter the interpretation of GeneChip data. *Nucleic Acids Res.* **33**, e175.
- de Folter, S. and Angenent, G. C. (2006). trans meets cis in MADS science. *Trends Plant Sci.* **11**, 224-231.
- de Folter, S. and Immink, R. G. H. (2011). Yeast protein-protein interaction assays and screens. *Methods Mol. Biol.* **754**, 145-165.
- de Folter, S., Immink, R. G., Kieffer, M., Parenicova, L., Henz, S. R., Weigel, D., Busscher, M., Kooiker, M., Colombo, L., Kater, M. M. et al. (2005). Comprehensive interaction map of the *Arabidopsis* MADS box transcription factors. *Plant Cell* **17**, 1424-1433.
- de Folter, S., Shchennikova, A. V., Franken, J., Busscher, M., Baskar, R., Grossniklaus, U., Angenent, G. C. and Immink, R. G. H. (2006). A Bsister MADS-box gene involved in ovule and seed development in petunia and *Arabidopsis*. *Plant J.* **47**, 934-946.
- Delp, G. and Palva, E. T. (1999). A novel flower-specific *Arabidopsis* gene related to both pathogen-induced and developmentally regulated plant beta-1,3-glucanase genes. *Plant Mol. Biol.* **39**, 565-575.
- Delude, C., Moussu, S., Joubès, J., Ingram, G. and Domergue, F. (2016). Plant surface lipids and epidermis development. *Subcell. Biochem.* **86**, 287-313.
- Dresselhaus, T. and Franklin-Tong, N. (2013). Male-female crosstalk during pollen germination, tube growth and guidance, and double fertilization. *Mol. Plant* **6**, 1018-1036.
- Esquer, I., Mizziotti, C., Nguema-Ona, E., Gotté, M., Beauzamy, L., Viana, V. E., Dubrulle, N., Costa de Oliveira, A., Caporali, E., Koroney, A.-S. et al. (2016). The developmental regulator SEEDSTICK controls structural and mechanical properties of the *Arabidopsis* seed coat. *Plant Cell* **28**, 2478-2492.
- Favaro, R., Pinyopich, A., Battaglia, R., Kooiker, M., Borghi, L., Ditta, G., Yanofsky, M. F., Kater, M. M. and Colombo, L. (2003). MADS-box protein complexes control carpel and ovule development in *Arabidopsis*. *Plant Cell* **15**, 2603-2611.
- Ferrándiz, C., Fourquin, C., Prunet, N., Scutt, C. P., Sundberg, E., Trehin, C. and Vialette-Guiraud, A. C. M. (2010). Carpel development. *Adv. Bot. Res.* **55**, 1-73.
- Fujisawa, M., Nakano, T. and Ito, Y. (2011). Identification of potential target genes for the tomato fruit-ripening regulator RIN by chromatin immunoprecipitation. *BMC Plant Biol.* **11**, 26.
- Fujisawa, M., Shima, Y., Nakagawa, H., Kitagawa, M., Kimbara, J., Nakano, T., Kasumi, T. and Ito, Y. (2014). Transcriptional regulation of fruit ripening by tomato FRUITFULL homologs and associated MADS box proteins. *Plant Cell* **26**, 89-101.
- Fukuchi-Mizutani, M., Tasaka, Y., Tanaka, Y., Ashikari, T., Kusumi, T. and Murata, N. (1998). Characterization of delta 9 acyl-lipid desaturase homologues from *Arabidopsis thaliana*. *Plant Cell Physiol.* **39**, 247-253.
- Gapper, N. E., McQuinn, R. P. and Giovannoni, J. J. (2013). Molecular and genetic regulation of fruit ripening. *Plant Mol. Biol.* **82**, 575-591.
- Gómez, M. D., Vera-Sirera, F. and Pérez-Amador, M. A. (2014). Molecular programme of senescence in dry and fleshy fruits. *J. Exp. Bot.* **65**, 4515-4526.
- González-Morales, S. I., Chávez-Montes, R. A., Hayano-Kanashiro, C., Alejo-Jacuinde, G., Rico-Cambren, T. Y., de Folter, S. and Herrera-Estrella, L. (2016). Regulatory network analysis reveals novel regulators of seed desiccation tolerance in *Arabidopsis thaliana*. *Proc. Natl. Acad. Sci. USA* **113**, E5232-E5241.
- Gremski, K., Ditta, G. and Yanofsky, M. F. (2007). The HECATE genes regulate female reproductive tract development in *Arabidopsis thaliana*. *Development* **134**, 3593-3601.
- Han, Y.-C., Fu, C.-C., Kuang, J.-F., Chen, J.-Y. and Lu, W.-J. (2016). Two banana fruit ripening-related C2H2 zinc finger proteins are transcriptional repressors of ethylene biosynthetic genes. *Postharvest Biol. Technol.* **116**, 8-15.
- He, H., Bai, M., Tong, P., Hu, Y., Yang, M. and Wu, H. (2018). CELLULASE6 and MANNANASE7 affect cell differentiation and silique dehiscence. *Plant Physiol.* **176**, 2186-2201.
- Heilmann, I., Pidkowich, M. S., Girke, T. and Shanklin, J. (2004). Switching desaturase enzyme specificity by alternate subcellular targeting. *Proc. Natl. Acad. Sci. USA* **101**, 10266-10271.
- Heisler, M. G., Atkinson, A., Bylstra, Y. H., Walsh, R. and Smyth, D. R. (2001). SPATULA, a gene that controls development of carpel margin tissues in *Arabidopsis*, encodes a bHLH protein. *Development* **128**, 1089-1098.
- Hepler, P. K., Rounds, C. M. and Winship, L. J. (2013). Control of cell wall extensibility during pollen tube growth. *Mol. Plant* **6**, 998-1017.
- Herrera-Ubaldo, H. and de Folter, S. (2018). Exploring cell wall composition and modifications during the development of the gynoecium medial domain in *Arabidopsis*. *Frontier. Plant Sci.* **9**, 454.
- Honma, T. and Goto, K. (2001). Complexes of MADS-box proteins are sufficient to convert leaves into floral organs. *Nature* **409**, 525-529.
- Immink, R. G. H., Tonaco, I. A. N., de Folter, S., Shchennikova, A., van Dijk, A. D. J., Busscher-Lange, J., Borst, J. W. and Angenent, G. C. (2009). SEPALLATA3: the 'glue' for MADS box transcription factor complex formation. *Genome Biol.* **10**, R24.
- Itkin, M., Seybold, H., Breitel, D., Rogachev, I., Meir, S. and Aharoni, A. (2009). TOMATO AGAMOUS-LIKE 1 is a component of the fruit ripening regulatory network. *Plant J.* **60**, 1081-1095.
- James, P., Halladay, J. and Craig, E. A. (1996). Genomic libraries and a host strain designed for highly efficient two-hybrid selection in yeast. *Genetics* **144**, 1425-1436.
- Jiang, L., Yang, S. L., Xie, L. F., Puah, C. S., Zhang, X. Q., Yang, W. C., Sundaresan, V. and Ye, D. (2005). VANGUARD1 encodes a pectin methyltransferase that enhances pollen tube growth in the *Arabidopsis* style and transmitting tract. *Plant Cell* **17**, 584-596.
- Kang, J., Park, J., Choi, H., Burla, B., Kretzschmar, T., Lee, Y. and Martinioia, E. (2011). Plant ABC Transporters. *Arabidopsis Book* **9**, e0153.
- Karlova, R., Chapman, N., David, K., Angenent, G. C., Seymour, G. B. and de Maagd, R. A. (2014). Transcriptional control of fleshy fruit development and ripening. *J. Exp. Bot.* **65**, 4527-4541.
- Kaufmann, K., Anfang, N., Saedler, H. and Theissen, G. (2005). Mutant analysis, protein-protein interactions and subcellular localization of the *Arabidopsis* B sister (ABS) protein. *Mol. Genet. Genomics* **274**, 103-118.
- Knoester, M., van Loon, L. C., van den Heuvel, J., Hennig, J., Bol, J. F. and Linthorst, H. J. M. (1998). Ethylene-insensitive tobacco lacks nonhost resistance against soil-borne fungi. *Proc. Natl. Acad. Sci. USA* **95**, 1933-1937.
- Kooiker, M., Airoldi, C. A., Losa, A., Manzotti, P. S., Finzi, L., Kater, M. M. and Colombo, L. (2005). BASIC PENTACYSSTEINE1, a GA binding protein that induces conformational changes in the regulatory region of the homeotic *Arabidopsis* gene SEEDSTICK. *Plant Cell* **17**, 722-729.
- Krolkowski, K. A., Victor, J. L., Wagler, T. N., Lolle, S. J. and Pruitt, R. E. (2003). Isolation and characterization of the *Arabidopsis* organ fusion gene HOTHEAD. *Plant J.* **35**, 501-511.
- Kuijt, S. J. H., Lamers, G. E. M., Rueb, S., Scarpella, E., Ouwerkerk, P. B. F., Spaik, H. P. and Meijer, A. H. (2004). Different subcellular localization and trafficking properties of KNOX class 1 homeodomain proteins from rice. *Plant Mol. Biol.* **55**, 781-796.
- Lennon, K. A., Roy, S. E., Hepler, P. K. and Lord, E. M. (1998). The structure of the transmitting tissue of *Arabidopsis thaliana* (L.) and the path of pollen tube growth. *Sex. Plant Reprod.* **11**, 49-59.
- Li-Beisson, Y., Shorosh, B., Beisson, F., Andersson, M. X., Arondel, V., Bates, P. D., Baud, S., Bird, D., Debono, A., Durrett, T. P. et al. (2013). Acyl-lipid metabolism. *Arabidopsis Book* **11**, e0161.
- Livak, K. J. and Schmittgen, T. D. (2001). Analysis of relative gene expression data using real-time quantitative PCR and the 2(-Delta Delta C(T)) Method. *Methods* **25**, 402-408.
- Lolle, S. J. and Cheung, A. Y. (1993). Promiscuous germination and growth of wildtype pollen from *Arabidopsis* and related species on the shoot of the *Arabidopsis* mutant, fiddlehead. *Dev. Biol.* **155**, 250-258.
- Lolle, S. J., Hsu, W. and Pruitt, R. E. (1998). Genetic analysis of organ fusion in *Arabidopsis thaliana*. *Genetics* **149**, 607-619.
- Lombard, V., Golaconda Ramulu, H., Drula, E., Coutinho, P. M. and Henrissat, B. (2014). The carbohydrate-active enzymes database (CAZy) in 2013. *Nucleic Acids Res.* **42**, D490-D495.
- Losa, A., Colombo, M., Brambilla, V. and Colombo, L. (2010). Genetic interaction between AINTEGUMENTA (ANT) and the ovule identity genes SEEDSTICK (STK), SHATTERPROOF1 (SHP1) and SHATTERPROOF2 (SHP2). *Sex. Plant Reprod.* **23**, 115-121.
- Lozano-Sotomayor, P., Chávez Montes, R. A., Silvestre-Vañó, M., Herrera-Ubaldo, H., Greco, R., Pablo-Villa, J., Galliani, B. M., Diaz-Ramirez, D., Weemen, M., Boutilier, K. et al. (2016). Altered expression of the bZIP transcription factor DRINK ME affects growth and reproductive development in *Arabidopsis thaliana*. *Plant J.* **88**, 437-451.
- Luo, B., Xue, X.-Y., Hu, W.-L., Wang, L.-J. and Chen, X.-Y. (2007). An ABC transporter gene of *Arabidopsis thaliana*, AtWBC11, is involved in cuticle development and prevention of organ fusion. *Plant Cell Physiol.* **48**, 1790-1802.
- Mantegazza, O., Gregis, V., Mendes, M. A., Morandini, P., Alves-Ferreira, M., Patreze, C. M., Nardeli, S. M., Kater, M. M. and Colombo, L. (2014). Analysis of the *Arabidopsis* REM gene family predicts functions during flower development. *Ann. Bot.* **114**, 1507-1515.
- Marcus, S. E., Blake, A. W., Benians, T. A. S., Lee, K. J. D., Poyser, C., Donaldson, L., Leroux, O., Rogowski, A., Petersen, H. L., Boraston, A. et al.

- (2010). Restricted access of proteins to mannan polysaccharides in intact plant cell walls. *Plant J.* **64**, 191-203.
- Margolin, A. A., Nemenman, I., Basso, K., Wiggins, C., Stolovitzky, G., Dalla Favera, R. and Califano, A.** (2006a). ARACNE: an algorithm for the reconstruction of gene regulatory networks in a mammalian cellular context. *BMC Bioinformatics* **7** Suppl. 1, S7.
- Margolin, A. A., Wang, K., Lim, W. K., Kustagi, M., Nemenman, I. and Califano, A.** (2006b). Reverse engineering cellular networks. *Nat. Protoc.* **1**, 662-671.
- Marsch-Martínez, N. and de Folter, S.** (2016). Hormonal control of the development of the gynoecium. *Curr. Opin. Plant Biol.* **29**, 104-114.
- Marsch-Martínez, N., Zúñiga-Mayo, V. M., Herrera-Ubaldo, H., Ouwerkerk, P. B. F., Pablo-Villa, J., Lozano-Sotomayor, P., Greco, R., Ballester, P., Balanzà, V., Kuijt, S. J. H. et al.** (2014). The NTT transcription factor promotes replum development in Arabidopsis fruits. *Plant J.* **80**, 69-81.
- Matias-Hernandez, L., Battaglia, R., Galbati, F., Rubes, M., Eichenberger, C., Grossniklaus, U., Kater, M. M. and Colombo, L.** (2010). VERDANDI is a direct target of the MADS domain ovule identity complex and affects embryo sac differentiation in Arabidopsis. *Plant Cell* **22**, 1702-1715.
- Mauch-Mani, B. and Slusarenko, A. J.** (1994). Systemic acquired resistance in Arabidopsis thaliana induced by a predisposing infection with a pathogenic isolate of fusarium oxysporum. *Mol. Plant-Microbe Interact.* **7**, 378-383.
- Mendes, M. A., Guerra, R. F., Castelano, B., Silva-Velazquez, Y., Morandini, P., Manrique, S., Baumann, N., Gross-Hardt, R., Dickinson, H. and Colombo, L.** (2016). Live and let die: a REM complex promotes fertilization through synergid cell death in Arabidopsis. *Development* **143**, 2780-2790.
- Mizuta, Y. and Higashiyama, T.** (2018). Chemical signaling for pollen tube guidance at a glance. *J. Cell Sci.* **131**, jcs208447.
- Mizzotti, C., Mendes, M. A., Caporali, E., Schnittger, A., Kater, M. M., Battaglia, R. and Colombo, L.** (2012). The MADS box genes SEEDSTICK and ARABIDOPSIS Bsister play a maternal role in fertilization and seed development. *Plant J.* **70**, 409-420.
- Mizzotti, C., Ezquer, I., Paolo, D., Rueda-Romero, P., Guerra, R. F., Battaglia, R., Rogachev, I., Aharoni, A., Kater, M. M., Caporali, E. et al.** (2014). SEEDSTICK is a master regulator of development and metabolism in the arabidopsis seed coat. *PLoS Genet.* **10**, e1004856.
- Mollet, J.-C., Leroux, C., Dardelle, F. and Lehner, A.** (2013). Cell wall composition, biosynthesis and remodeling during pollen tube growth. *Plants (Basel)* **2**, 107-147.
- Nawrath, C.** (2006). Unraveling the complex network of cuticular structure and function. *Curr. Opin. Plant Biol.* **9**, 281-287.
- Nole-Wilson, S., Azhakanandam, S. and Franks, R. G.** (2010). Polar auxin transport together with aintegumenta and revoluta coordinate early Arabidopsis gynoecium development. *Dev. Biol.* **346**, 181-195.
- Ogawa, M., Kay, P., Wilson, S. and Swain, S. M.** (2009). ARABIDOPSIS DEHISCENCE ZONE POLYGALACTURONASE1 (ADPG1), ADPG2, and QUARTET2 are Polygalacturonases required for cell separation during reproductive development in Arabidopsis. *Plant Cell* **21**, 216-233.
- Pan, I. L., McQuinn, R., Giovannoni, J. J. and Irish, V. F.** (2010). Functional diversification of AGAMOUS lineage genes in regulating tomato flower and fruit development. *J. Exp. Bot.* **61**, 1795-1806.
- Panikashvili, D., Savaldi-Goldstein, S., Mandel, T., Yifhar, T., Franke, R. B., Hofer, R., Schreiber, L., Chory, J. and Aharoni, A.** (2007). The Arabidopsis DESPERADO/AtWBC11 transporter is required for cutin and wax secretion. *Plant Physiol.* **145**, 1345-1360.
- Panikashvili, D., Shi, J. X., Bocobza, S., Franke, R. B., Schreiber, L. and Aharoni, A.** (2010). The arabidopsis DSO/ABCG11 transporter affects cutin metabolism in reproductive organs and suberin in roots. *Mol. Plant* **3**, 563-575.
- Panikashvili, D., Shi, J. X., Schreiber, L. and Aharoni, A.** (2011). The Arabidopsis ABCG13 transporter is required for flower cuticle secretion and patterning of the petal epidermis. *New Phytol.* **190**, 113-124.
- Paz-Ares, J. and The REGIA Consortium.** (2002). REGIA, an EU project on functional genomics of transcription factors from Arabidopsis thaliana. *Comp. Funct. Genomics* **3**, 102-108.
- Persikov, A. V. and Singh, M.** (2014). De novo prediction of DNA-binding specificities for Cys2His2 zinc finger proteins. *Nucleic Acids Res.* **42**, 97-108.
- Pighin, J. A., Zheng, H. Q., Balakshin, L. J., Goodman, I. P., Western, T. L., Jetter, R., Kunst, L. and Samuels, A. L.** (2004). Plant cuticular lipid export requires an ABC transporter. *Science* **306**, 702-704.
- Pinyopich, A., Ditta, G. S., Savidge, B., Liljgren, S. J., Baumann, E., Wisman, E. and Yanofsky, M. F.** (2003). Assessing the redundancy of MADS-box genes during carpel and ovule development. *Nature* **424**, 85-88.
- Pruitt, R. E., Vielle-Calzada, J.-P., Ploense, S. E., Grossniklaus, U. and Lolle, S. J.** (2000). FIDDLEHEAD, a gene required to suppress epidermal cell interactions in Arabidopsis, encodes a putative lipid biosynthetic enzyme. *Proc. Natl. Acad. Sci. USA* **97**, 1311-1316.
- Reyes-Olalde, J. I., Zúñiga-Mayo, V. M., Chávez Montes, R. A., Marsch-Martínez, N. and de Folter, S.** (2013). Inside the gynoecium: at the carpel margin. *Trends Plant Sci.* **18**, 644-655.
- Reyes-Olalde, J. I., Zúñiga-Mayo, V. M., Serwatowska, J., Montes, R. A. C., Lozano-Sotomayor, P., Herrera-Ubaldo, H., Gonzalez-Aguilera, K. L., Ballester, P., Ripoll, J. J., Ezquer, I. et al.** (2017). The bHLH transcription factor SPATULA enables cytokinin signaling, and both activate auxin biosynthesis and transport genes at the medial domain of the gynoecium. *PLoS Genet.* **13**, e1006726.
- Roeder, A. H. K. and Yanofsky, M. F.** (2006). Fruit development in Arabidopsis. *Arabidopsis Book* **4**, e0075.
- Rohrmann, J., Tohge, T., Alba, R., Osorio, S., Caldana, C., McQuinn, R., Arvidsson, S., van der Merwe, M. J., Riaño-Pachón, D. M., Mueller-Roeber, B. et al.** (2011). Combined transcription factor profiling, microarray analysis and metabolite profiling reveals the transcriptional control of metabolic shifts occurring during tomato fruit development. *Plant J.* **68**, 999-1013.
- Serin, E. A. R., Nijveen, H., Hilhorst, H. W. M. and Ligterink, W.** (2016). Learning from co-expression networks: possibilities and challenges. *Front. Plant Sci.* **7**, 444.
- Shima, Y., Fujisawa, M., Kitagawa, M., Nakano, T., Kimbara, J., Nakamura, N., Shina, T., Sugiyama, J., Nakamura, T., Kasumi, T. et al.** (2014). Tomato FRUITFULL homologs regulate fruit ripening via ethylene biosynthesis. *Biosci. Biotechnol. Biochem.* **78**, 231-237.
- Smaczniak, C., Immink, R. G. H., Muino, J. M., Blanvillain, R., Busscher, M., Busscher-Lange, J., Dinh, Q. D., Liu, S., Westphal, A. H., Boeren, S. et al.** (2012). Characterization of MADS-domain transcription factor complexes in Arabidopsis flower development. *Proc. Natl. Acad. Sci. USA* **109**, 1560-1565.
- Smyth, D. R., Bowman, J. L. and Meyerowitz, E. M.** (1990). Early flower development in Arabidopsis. *Plant Cell* **2**, 755-767.
- Sotelo-Silveira, M., Cucinotta, M., Chauvin, A.-L., Chavez Montes, R. A., Colombo, L., Marsch-Martínez, N. and de Folter, S.** (2013). Cytochrome P450 CYP78A9 is involved in Arabidopsis reproductive development. *Plant Physiol.* **162**, 779-799.
- Stracke, R., Ishihara, H., Huep, G., Barsch, A., Mehrtens, F., Niehaus, K. and Weisshaar, B.** (2007). Differential regulation of closely related R2R3-MYB transcription factors controls flavonol accumulation in different parts of the Arabidopsis thaliana seedling. *Plant J.* **50**, 660-677.
- Tanaka, H. and Machida, Y.** (2007). *The Cuticle and Cellular Interactions Annual Plant Reviews Volume 23: Biology of the Plant Cuticle*. Blackwell Publishing Ltd.
- Tissier, A. F., Marillonnet, S., Klimyuk, V., Patel, K., Torres, M. A., Murphy, G. and Jones, J. D.** (1999). Multiple independent defective suppressor-mutator transposon insertions in Arabidopsis: a tool for functional genomics. *Plant Cell* **11**, 1841-1852.
- Trigueros, M., Navarrete-Gomez, M., Sato, S., Christensen, S. K., Pelaz, S., Weigel, D., Yanofsky, M. F. and Ferrandiz, C.** (2009). The NGATHA genes direct style development in the Arabidopsis gynoecium. *Plant Cell* **21**, 1394-1409.
- Ukitsu, H., Kuromori, T., Toyooka, K., Goto, Y., Matsuoka, K., Sakuradani, E., Shimizu, S., Kamiya, A., Imura, Y., Yuguchi, M. et al.** (2007). Cytological and biochemical analysis of COF1, an Arabidopsis mutant of an ABC transporter gene. *Plant Cell Physiol.* **48**, 1524-1533.
- van Dam, S., Vosa, U., van der Graaf, A., Franke, L. and de Magalhães, J. P.** (2017). Gene co-expression analysis for functional classification and gene-disease predictions. *Brief. Bioinform.* **19**, 575-592.
- Verger, S., Long, Y., Boudaoud, A. and Hamant, O.** (2018). A tension-adhesion feedback loop in plant epidermis. *eLife* **7**, e34460.
- Vrebalov, J., Ruezinsky, D., Padmanabhan, V., White, R., Medrano, D., Drake, R., Schuch, W. and Giovannoni, J.** (2002). A MADS-box gene necessary for fruit ripening at the tomato ripening-inhibitor (rin) locus. *Science* **296**, 343-346.
- Vrebalov, J., Pan, I. L., Arroyo, A. J. M., McQuinn, R., Chung, M., Poole, M., Rose, J., Seymour, G., Grandillo, S., Giovannoni, J. et al.** (2009). Fleshy fruit expansion and ripening are regulated by the Tomato SHATTERPROOF gene TAGL1. *Plant Cell* **21**, 3041-3062.
- Wellmer, F., Bowman, J. L., Davies, B., Ferrándiz, C., Fletcher, J. C., Franks, R. G., Graciet, E., Gregis, V., Ito, T., Jack, T. P. et al.** (2014). Flower development: open questions and future directions. In *Flower Development: Methods and Protocols* (ed. J. L. Riechmann and F. Wellmer), pp. 103-124. New York, NY: Springer New York.
- Weng, L., Zhao, F., Li, R., Xu, C., Chen, K. and Xiao, H.** (2015). The zinc finger transcription factor SIZFP2 negatively regulates abscisic acid biosynthesis and fruit ripening in tomato. *Plant Physiol.* **167**, 931-949.
- Wynn, A. N., Rueschhoff, E. E. and Franks, R. G.** (2011). Transcriptomic characterization of a synergistic genetic interaction during carpel margin meristem development in Arabidopsis thaliana. *PLoS ONE* **6**, e26231.
- Yao, K., Bacchetta, R. G., Lockhart, K. M., Friesen, L. J., Potts, D. A., Covello, P. S. and Taylor, D. C.** (2003). Expression of the Arabidopsis ADS1 gene in Brassica juncea results in a decreased level of total saturated fatty acids. *Plant Biotechnol. J.* **1**, 221-229.
- Yeats, T. H. and Rose, J. K. C.** (2013). The formation and function of plant cuticles. *Plant Physiol.* **163**, 5-20.
- Yephremov, A., Wisman, E., Huijser, P., Huijser, C., Wellesen, K. and Saedler, H.** (1999). Characterization of the FIDDLEHEAD gene of Arabidopsis reveals a link between adhesion response and cell differentiation in the epidermis. *Plant Cell* **11**, 2187-2201.

- Yu, X., Li, L., Zola, J., Aluru, M., Ye, H., Foudree, A., Guo, H., Anderson, S., Aluru, S., Liu, P. et al. (2011). A brassinosteroid transcriptional network revealed by genome-wide identification of BES1 target genes in *Arabidopsis thaliana*. *Plant J.* **65**, 634-646.
- Zúñiga-Mayo, V. M., Marsch-Martínez, N. and de Folter, S. (2012). JAIBA, a class-II HD-ZIP transcription factor involved in the regulation of meristematic activity, and important for correct gynoecium and fruit development in *Arabidopsis*. *Plant J.* **71**, 314-326.